Supporting Information for:

Metal-Diamidobenzoquinone Frameworks via Post-Synthetic Linker Exchange

Lujia Liu, Liang Li, Michael E. Ziebel, and T. David Harris*

Departments of Chemistry,

Northwestern University, 2145 Sheridan Road, Evanston, Illinois 60208, USA
University of California, Berkeley, California 94720, USA

Email: dharris@berkeley.edu

J. Am. Chem. Soc.

Table of Contents

Experimental Section

General Considerations. Unless otherwise specified, chemicals and solvents were purchased from commercial vendors and used without further purification. Deuterated solvents were purchased from Cambridge Isotope Laboratories. Dichloromethane (DCM) and benzene were dried using a commercial solvent purification system from Pure Process Technology. Water was obtained from a purification system from EMD Millipore. The compound $(Me_2NH_2)_2[Zn_2L_3]$ (**1**) was prepared according a literature procedure.[1] Elemental analysis was conducted by Midwest Microlab Inc. or Integrated Molecular Structure Education and Research Center (IMSERC) at Northwestern University.

2,5-Diamino-3,6-Dibromo-1,4-Benzoquinone ($H_2{}^{Br}L'$).[2] In a 250 mL round bottom flask, 2,3,5,6-tetrabromo-1,4-benzoquinone (*p*-bromanil, 25 g, 59 mmol) was suspended in ethanol (150 mL). The resulting suspension was heated to 60 °C and NH_4OH (30%, 200 mL) was added dropwise. The reaction mixture was heated at reflux for another 12 h. The brown solid was isolated by filtration, washed with water (200 mL), ethanol (200 mL), and diethyl ether (200 mL), and dried under reduced pressure to afford the title compound as a brown crystalline solid. Yield: 9.4 g (54%) ^{13}C NMR (125 MHz, DCl/DMSO-d_6): δ 170.12 (C=O), 150.55 (C-N), 90.17 (C-Br) ppm.

2,5-Diamino-3,6-Dichloro-1,4-Benzoquinone ($H_2{}^{Cl}L'$).[3] 2,3,5,6-tetrachloro-1,4-benzoquinone (*p*-chloranil, 23 g, 94 mmol) was suspended in methoxyethyl acetate (90 mL). The resulting yellow turbid suspension was heated to 60 °C and ammonium hydroxide (30%, 36 mL) was dropped slowly to the mixture. The reaction mixture was then kept at 80 °C for 1 h before cooled to room temperature and stirred for another 24 h. The brown solid was filtered, washed with water (100 mL) and acetone (50 mL), and dried under reduced pressure to afford the title compound as a brown crystalline solid. Yield 19 g (98%). ^{13}C NMR (125 MHz, DCl/DMSO-d_6) δ 170.13 (C=O), 148.67 (C-N), 99.41 (C-Cl) ppm.

$(Et_4N)_2[Zn_2L_{1.3}{}^{Br}L'_{1.7}]\cdot0.57DMF\cdot0.14Et_2O$ (2). In a 20 mL scintillation vial, $(NEt_4)OH$ (0.828 mL, 40% wt. in H_2O, 2.25 mmol) was added to a brown suspension of 2,5-diamino-3,6-dibromobenzoquinone ($H_2{}^{Br}L'$, 665 mg, 2.25 mmol) in DMF (15 mL) to form a dark purple solution. Purple hexagonal crystals of $(Me_2NH_2)_2[Zn_2L_3]$ (**1**, 41 mg, 50 μmol) standing in DMF (0.5 mL) were then added to this solution. The resulting mixture was heated to 75 °C in a heating block for 48 h. The supernatant was decanted while the reaction mixture was still hot. Fresh, ambient-temperature DMF (5 mL) was immediately added to the residual solid. At ambient temperature, this decanting-replenishing procedure was repeated 10 times, until the supernatant became colorless. The supernatant was again decanted and fresh Et_2O (5 mL) was added. This decanting-replenishing procedure was repeated 5 more times. After the final decanting of the supernatant, the residual solid product was heated to 100 °C under dynamic vacuum (4 mTorr) for 16.5 h to afford the title product as red hexagonal crystals. Yield: 60 mg (98%). ^1H NMR (500 MHz, DCl/DMSO-d_6, see Figure S12): δ 8.02 (s, $H_2{}^{Br}L'$), 7.85 (s, DMF), 3.85 (s, $H_2{}^{Br}L'$), 3.71 (H_3O^+), 3.37 (q, $J = 6.9$ Hz, Et_2O), 3.20 (q, $J = 7.4$ Hz, Et_4N^+), 2.88 (s, DMF), 2.72 (s, DMF), 1.15 (tt, $J = 7.4$ Hz, Et_4N^+), 1.08 (t, $J = 6.9$ Hz, Et_2O) ppm. ^{13}C NMR (125 MHz, DCl/DMSO-d_6, see Figure S10) δ 170.1 ($H_2{}^{Br}L'$, C=O), 165.8 (H_2L, C=O), 162.5 (DMF), 150.6 ($H_2{}^{Br}L'$, C-N), 109.1 (H_2L, C-Cl), 90.2 ($H_2{}^{Br}L'$, C-Br), 65.0 (Et_2O), 51.5 (Et_4N^+), 35.9 (DMF), 30.9 (DMF), 15.3 (Et_2O),

7.1 (Et_4N^+) ppm. Anal. Calcd. for [$C_{36.27}H_{48.79}Br_{3.4}Cl_{2.6}N_{5.97}O_{9.31}Zn_2$]: C, 35.94; H, 4.06; N, 6.90 %. Found: C, 36.49; H, 4.56; N, 7.25 %.

(Et_4N)$_2$[$Zn_2L_{1.1}{}^{Cl}L'_{1.9}$]·0.64$CH_2Cl_2$ (3). In a 20 mL scintillation vial, (NEt_4)OH (0.828 mL, 40% wt. in H_2O, 2.25 mmol) was added to a brown suspension of 2,5-diamino-3,6-dichlorobenzoquinone ($H_2{}^{Cl}L'$, 466 mg, 2.25 mmol) in DMF (15 mL) to form a dark purple solution. Purple hexagonal crystals of (Me_2NH_2)$_2$[$Zn_2(L)_3$] (**1**, 41 mg, 50 μmol) standing in DMF (0.5 mL) were then added to this solution. The resulting mixture was heated to 75 °C in a heating block for 48 h. The supernatant was decanted while the reaction mixture was still hot. Fresh, ambient-temperature DMF (5 mL) was immediately added to the residual solid. At ambient temperature, this decanting-replenishing procedure was repeated 10 times, until the supernatant became colorless. The supernatant was again decanted and fresh CH_2Cl_2 (5 mL) was added. This decanting-replenishing procedure was repeated 5 more times. After the final decanting of the supernatant, the residual solid product was heated to 100 °C under dynamic vacuum (4 mTorr) for 2 h to afford the title product as red hexagonal crystals. Yield: 50 mg (97%). ^{1}H NMR (500 MHz, DCl/DMSO-d$_6$, see Figure S13): δ 8.01 (s, $H_2{}^{Cl}L'$), 8.00 (s, $H_2{}^{Cl}L'$), 5.75 (s, CH_2Cl_2), 3.20 (q, $J = 7.4$ Hz, Et_4N^+), 1.16 (tt, $J = 7.4$ Hz, Et_4N^+) ppm. ^{13}C NMR (125 MHz, DCl/DMSO-d$_6$, see Figure S11) δ 170.1 ($H_2{}^{Cl}L'$, C=O), 165.7 (H_2L, C=O), 148.7 ($H_2{}^{Cl}L'$, C-N), 108.7 (H_2L, C-Cl), 99.4 ($H_2{}^{Cl}L'$, C-Cl), 54.9 (CH_2Cl_2), 51.4 (Et_4N^+), 7.1 (Et_4N^+) ppm. For combustion elemental analysis, the crystals were further heated at 100 °C under dynamic vacuum (4 mTorr) for 14 hours to afford a solvent-free sample with a formula of (Et_4N)$_2$[$Zn_2(L)_{1.1}({}^{Cl}L')_{1.9}$]. Anal. Calcd. for [$C_{34}H_{43.8}Cl_6N_{5.8}O_{8.2}Zn_2$]: C, 40.50; H, 4.38; N, 8.06 %. Found: C, 40.41; H, 4.69; N, 7.88 %.

(Me_2NH_2)$_2$[Mn_2L_3] (4). To a solid mixture of Mn(NO_3)$_2$·4H_2O (4.0 g, 16 mmol) and chloranilic acid (H_2L, 6.6 g, 32 mmol) in a 100 mL Schott bottle, DMF (80 mL) and H_2O (2.3 mL) were added. The resulting mixture was shaken until most of the solid dissolved, and the reaction was placed in an isothermal oven at 130 °C for 16 h. After the reaction mixture was cooled to ambient temperature, the mother liquor was decanted and then replenished with fresh DMF (50 mL). This decanting-replenishing procedure was repeated 10 times, until the supernatant became colorless. The supernatant was again decanted and fresh CH_2Cl_2 (50 mL) added. This decanting-replenishing procedure was repeated 5 more times. After final decanting of the supernatant, the residual solid product was heated to 100 °C under dynamic vacuum (4 mTorr) for 16.5 hours to afford the title product as brown hexagonal crystals. Yield: 3.1 g (47%). Anal. Calcd. for [$C_{22}H_{16}Cl_6Mn_2N_2O_{12}$]: C, 32.11; H, 1.96; N, 3.40 %. Found: C, 32.06; H, 2.21; N, 3.39 %.

(Et_4N)$_2$[$Mn_2L_{1.8}{}^{Br}L'_{1.2}$]·0.65DMF (5). In a 20 mL scintillation vial, (NEt_4)OH (0.828 mL, 40% wt. in H_2O, 2.25 mmol) was added to a brown suspension of 2,5-diamino-3,6-dibromobenzoquinone ($H_2{}^{Br}L'$, 665 mg, 2.25 mmol) in DMF (15 mL) to form a dark purple solution. Brown hexagonal crystals of (Me_2NH_2)$_2$[Mn_2L_3] (**4**, 41 mg, 50 μmol) standing in DMF (0.5 mL) were then added to this solution. The resulting mixture was heated to 75 °C in a heating block for 48 h. The supernatant was decanted while the reaction mixture was still hot. Fresh, ambient-temperature DMF (5 mL) was immediately added to the residual solid. At ambient temperature, this decanting-replenishing procedure was repeated 10 times, until the supernatant became colorless. The supernatant was again decanted and fresh CH_2Cl_2 (5 mL) was added. This

decanting-replenishing procedure was repeated 5 more times. After the final decanting of the supernatant, the residual solid product was heated to 80 °C under dynamic vacuum (49 mTorr) for 12 h to afford the title product as brown hexagonal crystals. Yield: 53 mg (97%). Anal. Calcd. for [$C_{35.95}H_{46.95}Br_{2.4}Cl_{3.6}Mn_2N_{5.05}O_{10.25}$]: C, 37.77; H, 4.14; N, 6.19 %. Found: C, 37.70; H, 4.21; N, 6.19 %.

($Et_4N)_2[Mn_2L_{1.5}{}^{Cl}L'_{1.5}$] (6). In a 20 mL scintillation vial, (NEt_4)OH (0.828 mL, 40% wt. in H_2O, 2.25 mmol) was added to a brown suspension of 2,5-diamino-3,6-dichlorobenzoquinone ($H_2{}^{Cl}L'$, 466 mg, 2.25 mmol) in DMF (15 mL) to form a dark purple solution. Brown hexagonal crystals of ($Me_2NH_2)_2[Mn_2L_3]$ (**4**, 41 mg, 50 μmol) standing in DMF (0.5 mL) were then added to this solution. The resulting mixture was heated to 75 °C in a heating block for 48 h. The supernatant was decanted while the reaction mixture was still hot. Fresh, ambient-temperature DMF (5 mL) was immediately added to the residual solid. At ambient temperature, this decanting-replenishing procedure was repeated 10 times, until the supernatant became colorless. The supernatant was again decanted and fresh CH_2Cl_2 (5 mL) was added. This decanting-replenishing procedure was repeated 5 more times. After the final decanting of the supernatant, the residual solid product was heated to 100 °C under dynamic vacuum (5 mTorr) for 13 h to afford the title product as brown hexagonal crystals. Yield: 48 mg (97%). Anal. Calcd. for [$C_{34}H_{43}Cl_6Mn_2N_5O_9$]: C, 41.32; H, 4.39; N, 7.09 %. Found: C, 41.74; H, 4.77; N, 7.00 %.

Single-Crystal X-ray Structure Determination. Single crystals of **2**–**6** were immersed in DMF to keep the compounds solvated before they were coated with a small amount of Paratone oil for data collection. Data collections were performed on one of the three following Bruker Kappa Apex II diffractometers, all of which are equipped with a Bruker Kappa APEX CCD area detector. The first diffractometer is equipped with a Cu Kα microfocus source and a MX optics monochromator. The second diffractometer is equipped with a switchable duo source with both Cu Kα and Mo Kα microfocus sources, both of which are monochromated with a corresponding Quazar optics. The third diffractometer is equipped Mo Kα sealed tube source and a graphite monochromator. The data collections were performed at 100 K or 250 K. Raw data were integrated, scaled and averaged using the Bruker APEX3 software.[4] Absorption corrections were applied using SADABS.[5] Space groups were determined by examination of systematic absence, *E*-statistics using XPREP[6] and successive refinement of structures. Structures were solved using SHELXT[7] and refined with SHELXL[7] using the Olex 2 graphical interface.[8] All framework atoms were solved and refined anisotropically. For **2**, **3**, **5**, and **6**, both diamino- and dihydroxobenzoquinone linkers are disordered by occupying the same lattice sites. To finalize the structure refinements, residual electron densities contributed from disordered solvent molecules and counterions were removed using the solvent mask protocol in Olex 2.[8] Crystallographic data and the details of data collection are listed in Table S1.

Powder X-ray Diffraction Analyses. Approximately 1 mg of polycrystalline samples were loaded in a hollow metallic sample holder, and both sides were sealed with Kapton tape. A small amount of extra DMF was added to the sample to ensure the samples were kept fully-solvated during the measurement. The powder X-ray diffraction (PXRD) patterns were measured at a transmission geometry using a STOE STADI MP instrument equipped with a Cu Kα_1 sealed tube

source and a 1D strip detector covering 2θ range of 6°. The sample holder was spun during the measurement to obtain a better powdered-average.

Raman Spectroscopy and Mapping. Crystals of **1**–**6** were deposited onto a silicon oxide-coated silicon wafer and sealed in a Linkam THMS350 V microscope stage. Raman spectra were collected using a Horiba LabRam HR Evolution confocal microscope. Individual crystals were excited with a 473 nm continuous-wave diode laser at 0.236 mW power equipped with a long working distance 50× microscope objective (NA = 0.50; Nikon) and 600 grooves/mm grating. To perform Raman mapping, a full spectrum at the energy range of 400–2000 cm^{-1} was collected at each mapping point. Intensities at 1550 cm^{-1} and 1612 cm^{-1} are chosen to probe the populations of $^{Cl}L'^{2-}$ and L^{2-}, respectively.

Qualitative NMR Spectroscopy. Samples were digested using the following protocol: 23 µL of a 35% DCl solution in D_2O was mixed with 1 mL of DMSO-d_6 to give a DCl/DMSO-d_6 stock solution. Approximately 2 mg of compound was digested in 150 µL of this stock solution and 450 µL of DMSO-d_6. ^1H and ^{13}C NMR spectra were then acquired immediately following dissolution using a Bruker Avance III 500 MHz spectrometer equipped with a DCH CryoProbe.

Quantitative ^{13}C NMR Spectroscopy. External ratiometric calibration curves were acquired for $H_2L/H_2{}^{Br}L'$ and $H_2L/H_2{}^{Cl}L'$ mixtures with known relative mole ratio. Specifically, qualitative ^{13}C NMR spectra were collected, and peaks were integrated using automatic method with MestReNova software package. Integral regions were detected automatically using Peak Picking algorithm with a minimum area threshold of 3%. Total peak area ratio for the two linkers are plotted against their mole ratios. Then, to quantify linker exchange in **2** and **3**, we integrated the peaks of their qualitative ^{13}C NMR spectra. The total peak area ratio for the two linkers were thus obtained, and linker ratios are found from external radiometric calibration curves.

Scanning Electron Microscopy and Energy Dispersive X-ray Spectroscopy. Desolvated crystals were sprinkled on a double-sided carbon tape which is fixed on a sample holder. To improve the electronic conductivity of the MOF crystals, samples were coated with carbon using a Denton III Desk Sputter Coater or osmium using a SPI Osmium Coater. Scanning electron imaging and EDX analyses were carried out using Hitachi S4800-II cFEG SEM or Hitachi SU8030 SEM. EDX data were acquired and analyzed using the Aztec software package. In the software, the samples were selected to have been coated with 100 nm of carbon regardless of the actual coating to attenuate the carbon signal to obtain a more accurate quantitation for metal and chlorine. The accelerating voltage was set to 30.0 kV to maximize the penetration. This led to an increase in the interaction volume of the electron beam with the interior of the sample, and therefore the EDX analysis reflected more interior of the sample rather than the outer surface.

Acid-Base Titration. Three ligand solutions were prepared by dissolving H_2L (21 mg, 0.10 mmol), $H_2{}^{Br}L'$ (9 mg, 0.030 mmol), or $H_2{}^{Cl}L'$ (15 mg, 0.072 mmol) in DMF (8 mL). To these solutions, aqueous NaOH solutions (0.02 mol/L) were added and pH values were measured using a Fisherbrand Accumet AB15 pH meter. Values of pK_{a1} were calculated based on the pH values prior to the addition of NaOH (see main text for details). For each ligand, up to 2 equivalents of

NaOH was added. A blank titration curve was prepared by gradually adding up to 0.5 mL of NaOH aqueous solution in DMF (3 mL).

N$_2$ Adsorption and Desorption. DMF-solvated samples were soaked in 10 mL of CH_2Cl_2 for at least 48 h, during which the solvent was decanted and replaced with fresh CH_2Cl_2 five times. The samples were pre-activated under vacuum for 3 h, transferred to an MBraun Ar glovebox, and loaded into pre-weighed borosilicate measurement tubes capped with Micromeritics *Transeals*. The samples were then placed under vacuum at 80 °C on a Micromeritics ASAP 2420 gas adsorption analyzer until the outgas rate was less than 2 μbar/min, typically 24 to 48 h. The evacuated sample tubes were then re-weighed to determine the mass of the activated samples and were transferred to the analysis ports of the instrument. N$_2$ adsorption and desorption isotherms were measured at 77 K using a liquid N$_2$ bath, and surface area were calculated using Brunauer-Emmett-Teller (BET) model.

Table S1 | Crystallographic data for MOFs **2**-**6**.
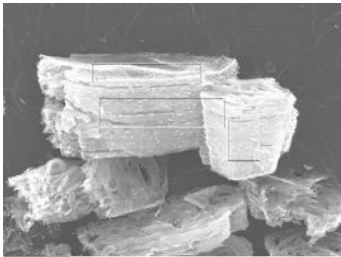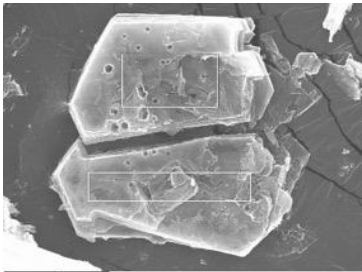
MOF[a]	$(Et_4N)_2[Zn_2L_{1.3}{}^{Br}L'_{1.7}]$ (**2**)	$(Et_4N)_2[Zn_2L_{1.1}{}^{Cl}L'_{1.9}]$ (**3**)	$(Me_2NH_2)_2[Mn_2L_3]$ (**4**)	$(Et_4N)_2[Mn_2L_{1.8}{}^{Br}L'_{1.2}]$ (**5**)	$(Et_4N)_2[Mn_2L_{1.5}{}^{Cl}L'_{1.5}]$ (**6**)
Empirical formula	$C_{34}H_{43.4}Br_{3.4}Cl_{2.6}N_{5.4}O_{8.6}Zn_2$	$C_{32}H_{43.8}Cl_6N_{5.8}O_{8.2}Zn_2$	$C_{22}H_{16}Cl_6Mn_2N_2O_{12}$	$C_{34}H_{42.4}Br_{2.4}Cl_{3.6}Mn_2N_{4.4}O_{9.6}$	$C_{34}H_{43}Cl_6Mn_2N_5O_9$
Formula weight	1159.99	1008.43	822.98	1095.65	988.35
Temperature/K	99.99	99.99	250.01	100.02	99.99
Crystal system	trigonal	trigonal	trigonal	trigonal	trigonal
Space group	P-31m	P-31m	P-31m	P-31m	P-31m
a, b/Å	13.9416(16)	13.9533(10)	14.017(4)	14.1160(5)	14.1380(11)
c/Å	10.2616(12)	10.1333(11)	8.970(2)	9.9697(10)	10.1420(12)
Volume/Å^3	1727.3(4)	1708.6(3)	1526.3(9)	1720.4(2)	1755.6(3)
Z	0.99996	0.99996	0.99996	0.99996	0.99996
ρ_{calc}g/cm^3	1.115	0.980	0.895	1.057	0.935
μ/mm^{-1}	2.795	3.313	0.708	6.205	5.316
F(000)	577.0	516.0	410.0	549.0	506.0
Crystal size/mm^3	0.091×0.085×0.011	0.196×0.136×0.07	0.26×0.192×0.162	0.6×0.5×0.1	0.346×0.307×0.122
Radiation	MoKα (λ = 0.71073)	CuKα (λ = 1.54178)	MoKα (λ = 0.71073)	CuKα (λ = 1.54178)	CuKα (λ = 1.54178)
2θ range	5.21 to 41.606	11.396 to 94.358	5.648 to 41.578	11.452 to 100.974	11.328 to 94.22
Index ranges	$-13 \leq h \leq 13$ $-13 \leq k \leq 13$ $-10 \leq l \leq 10$	$-13 \leq h \leq 13$ $-12 \leq k \leq 11$ $-9 \leq l \leq 9$	$-13 \leq h \leq 13$ $-13 \leq k \leq 14$ $-8 \leq l \leq 8$	$-14 \leq h \leq 8$ $-10 \leq k \leq 13$ $-9 \leq l \leq 9$	$-9 \leq h \leq 12$ $-13 \leq k \leq 9$ $-9 \leq l \leq 9$
Total/independent reflections	10580/668	7875/570	10280/572	2931/658	7061/589
Data/restraints/parameters	668/28/71	570/36/71	572/9/48	658/40/75	589/12/38
Goodness-of-fit	1.065	1.399	2.113	1.283	1.841
Final R indexes [I>=2σ (I)]	R_1 = 0.0632[b]; wR_2 = 0.1768[c]	R_1 = 0.1125; wR_2 = 0.3075	R_1 = 0.1492; wR_2 = 0.3761	R_1 = 0.0962; wR_2 = 0.2713	R_1 = 0.1680; wR_2 = 0.4226
Final R indexes [all data]	R_1 = 0.0917; wR_2 = 0.1966	R_1 = 0.1373; wR_2 = 0.3324	R_1 = 0.1590; wR_2 = 0.4383	R_1 = 0.1197; wR_2 = 0.3105	R_1 = 0.1924; wR_2 = 0.4455
Largest diff. peak/hole / e Å^{-3}	0.65/-0.41	1.19/-0.42	1.68/-0.53	0.76/-0.63	2.10/-0.55

[a]The discrepancy of the formulae is due to the SC-XRD experimental procedure that involves in soaking crystals in DMF, as detailed above

[b]$R_1 = \Sigma||F_0| - |F_C||/\Sigma|F_0|$

[c]$wR_2 = [\Sigma w(F_0{}^2 - F_C{}^2)^2/\Sigma w(F_o{}^2)^2]^{1/2}$

Table S2 | EDX spectra for $(Et_4N)_2[Mn_2L_{1.8}{}^{Br}L'_{1.2}]\cdot0.65DMF$ (**5**, batch 1)
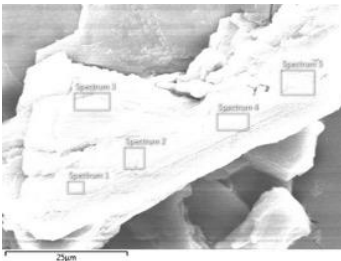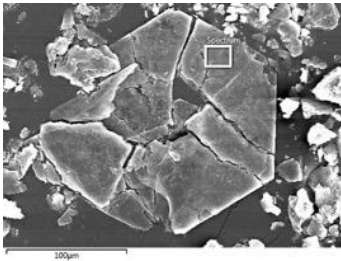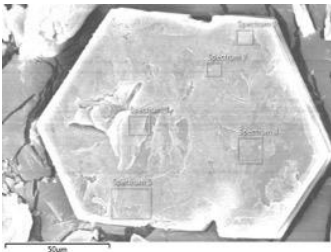
Spectrum	Br%[a]	Cl%[a]	Mn%[a]	Br:(Br+Cl)	Electron Image
1	25.0	51.8	23.2	0.326 : 1	
2	28.5	49.3	22.2	0.366 : 1	
3	27.9	50.2	21.9	0.357 : 1	
4	29.4	47.5	23.1	0.383 : 1	
5	28.7	48.4	22.9	0.372 : 1	
6	29.4	48.1	22.5	0.380 : 1	
7	28.2	49.2	22.6	0.364 : 1	
8	27.3	50.0	22.7	0.353 : 1	
9	31.4	47.4	21.2	0.398 : 1	
10	32.4	46.0	21.5	0.413 : 1	
11	33.8	44.3	21.8	0.433 : 1	
12	32.6	45.1	22.3	0.420 : 1	
13	31.1	47.5	21.4	0.396 : 1	
14	37.0	39.6	23.4	0.483 : 1	
15	31.7	46.3	22.0	0.406 : 1	
16	33.5	44.2	22.3	0.431 : 1	
17	30.7	44.1	25.2	0.410 : 1	

18	30.8	44.8	24.3	0.407 : 1	
19	28.4	47.0	24.5	0.377 : 1	
20	31.7	43.3	25.1	0.423 : 1	
21	28.9	46.3	24.8	0.385 : 1	
22	31.9	42.8	25.3	0.427 : 1	
23	29.4	46.3	24.3	0.389 : 1	
24	29.3	46.1	24.6	0.389 : 1	
Average	30.4	46.5	23.1	0.395 : 1	
STD	2.72	1.32	2.52	0.033 : 1	
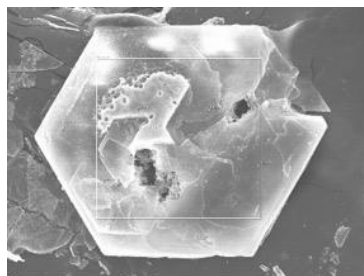
[a]Mole percentage, Cl + Mn + Co = 100%, same below.

Table S3 | EDX spectra for $(Et_4N)_2[Mn_2L_{1.8}{}^{Br}L'_{1.2}]$ (**5**, batch 2)

Spectrum	Br%	Cl%	Mn%	Br:(Br+Cl)	Electron Image
1	31.2	46.2	22.6	0.403 : 1	
2	30.8	45.5	23.7	0.404 : 1	
3	32.2	44.8	23.0	0.418 : 1	
4	31.1	45.5	23.4	0.406 : 1	
5	32.1	43.8	24.1	0.423 : 1	
6	31.4	43.3	25.3	0.420 : 1	
7	30.7	43.7	25.5	0.413 : 1	
8	29.9	44.1	26.0	0.404 : 1	
9	31.8	42.6	25.6	0.427 : 1	
10	31.9	41.3	26.7	0.436 : 1	
11	27.5	45.8	26.7	0.375 : 1	
12	29.1	43.4	27.5	0.402 : 1	
13	26.9	46.5	26.6	0.367 : 1	
14	25.0	48.5	26.5	0.340 : 1	
15	28.1	48.3	23.6	0.368 : 1	
16	31.9	43.2	24.9	0.425 : 1	
17	27.4	45.2	27.3	0.377 : 1	
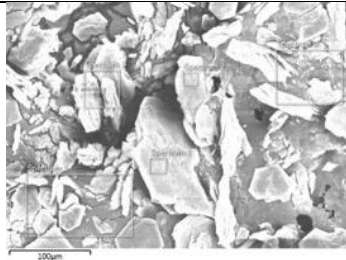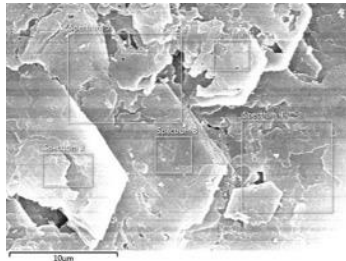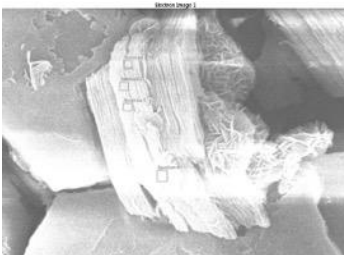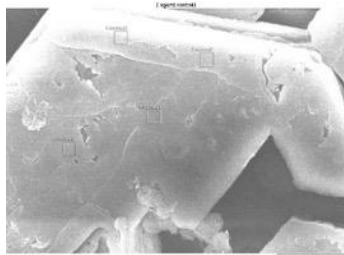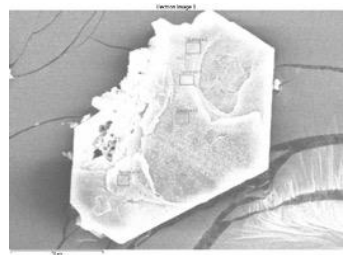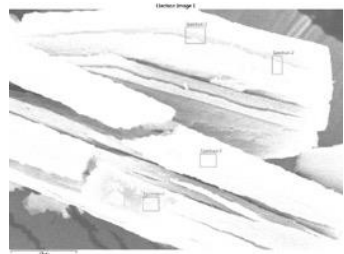
18	30.3	42.1	27.5	0.418 : 1	
19	29.1	43.3	27.3	0.404 : 1	
20	28.9	42.1	29.0	0.407 : 1	
21	29.5	44.0	26.5	0.401 : 1	
22	30.4	44.7	25.0	0.404 : 1	
23	28.4	44.9	26.7	0.387 : 1	
24	30.0	44.7	25.3	0.402 : 1	
25	28.8	44.4	26.8	0.393 : 1	
Average	29.8	44.5	25.7	0.401 : 1	
STD	1.86	1.75	1.63	0.022 : 1	

Table S4 | EDX spectra for $(Et_4N)_2[Mn_2L_{1.8}{}^{Br}L'_{1.2}]\cdot0.65DMF$ (**5**, batch 3)

Spectrum	Br%	Cl%	Mn%	Br:(Br+Cl)	Electron Image
1	24.6	44.6	30.8	0.356 : 1	
2	26.0	44.2	30.0	0.370 : 1	
3	26.4	43.1	30.4	0.380 : 1	
4	21.2	45.9	32.9	0.316 : 1	
5	33.6	41.4	25.0	0.448 : 1	
6	33.6	42.6	23.8	0.441 : 1	
7	30.4	40.4	29.1	0.429 : 1	
8	28.6	40.7	30.6	0.413 : 1	
9	32.3	39.2	28.5	0.451 : 1	
10	34.7	38.6	26.7	0.473 : 1	
11	31.4	42.4	26.2	0.425 : 1	
12	32.6	40.3	27.1	0.448 : 1	
13	26.3	44.7	28.9	0.370 : 1	
14	25.7	45.9	28.4	0.358 : 1	
15	24.4	46.5	29.1	0.344 : 1	
16	22.6	46.2	31.2	0.328 : 1	
17	30.3	41.3	28.4	0.423 : 1	
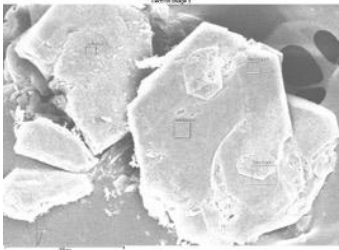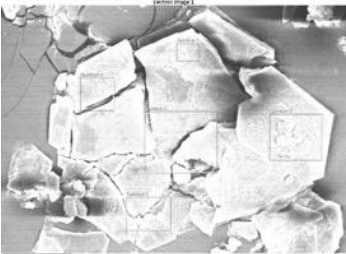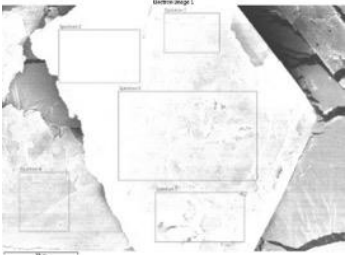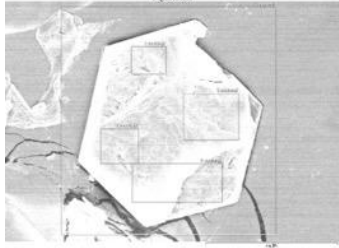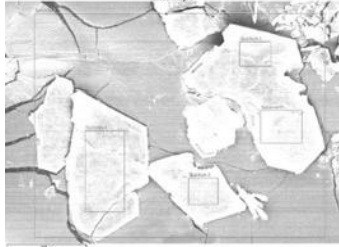
18	33.6	41.1	25.2	0.450 : 1	
19	34.0	40.8	25.2	0.455 : 1	
20	30.5	40.3	29.2	0.431 : 1	
Average	29.7	42.0	28.3	0.406 : 1	
STD	4.18	2.48	2.40	0.048 : 1	

Table S5 | EDX spectra for $(Et_4N)_2[Mn_2L_{1.8}{}^{Br}L'_{1.2}]\cdot 0.65DMF$ (**5**, batch 4)

Spectrum	Br%	Cl%	Mn%	Br:(Br+Cl)	Electron Image
1	20.9	39.1	39.9	0.348 : 1	
2	29.1	43.0	27.8	0.404 : 1	
3	28.6	42.9	28.6	0.400 : 1	
4	30.8	44.1	25.2	0.411 : 1	
5	30.6	41.9	27.4	0.408 : 1	
6	28.4	41.2	30.4	0.408 : 1	
7	25.9	40.7	33.3	0.389 : 1	
8	25.5	41.5	33.0	0.380 : 1	
9	28.5	43.0	28.5	0.398 : 1	
10	25.8	41.9	32.3	0.381 : 1	
11	31.0	44.2	24.8	0.412 : 1	
12	30.6	45.1	24.3	0.404 : 1	
13	34.6	40.4	25.0	0.462 : 1	
14	30.9	41.5	27.6	0.427 : 1	
15	29.3	44.0	26.7	0.400 : 1	
16	29.0	43.8	27.2	0.398 : 1	
17	30.1	44.6	25.3	0.403 : 1	

18	27.8	45.0	27.2	0.382 : 1	
19	28.5	43.6	27.9	0.395 : 1	
20	29.1	43.6	27.2	0.400 : 1	
21	28.6	44.0	27.4	0.393 : 1	
22	30.1	44.1	25.7	0.406 : 1	
23	29.5	43.6	26.8	0.404 : 1	
24	28.9	44.7	26.4	0.393 : 1	
25	29.5	43.2	27.2	0.406 : 1	
Average	28.7	43.1	28.2	0.401 : 1	
STD	2.50	1.56	3.42	0.020 : 1	
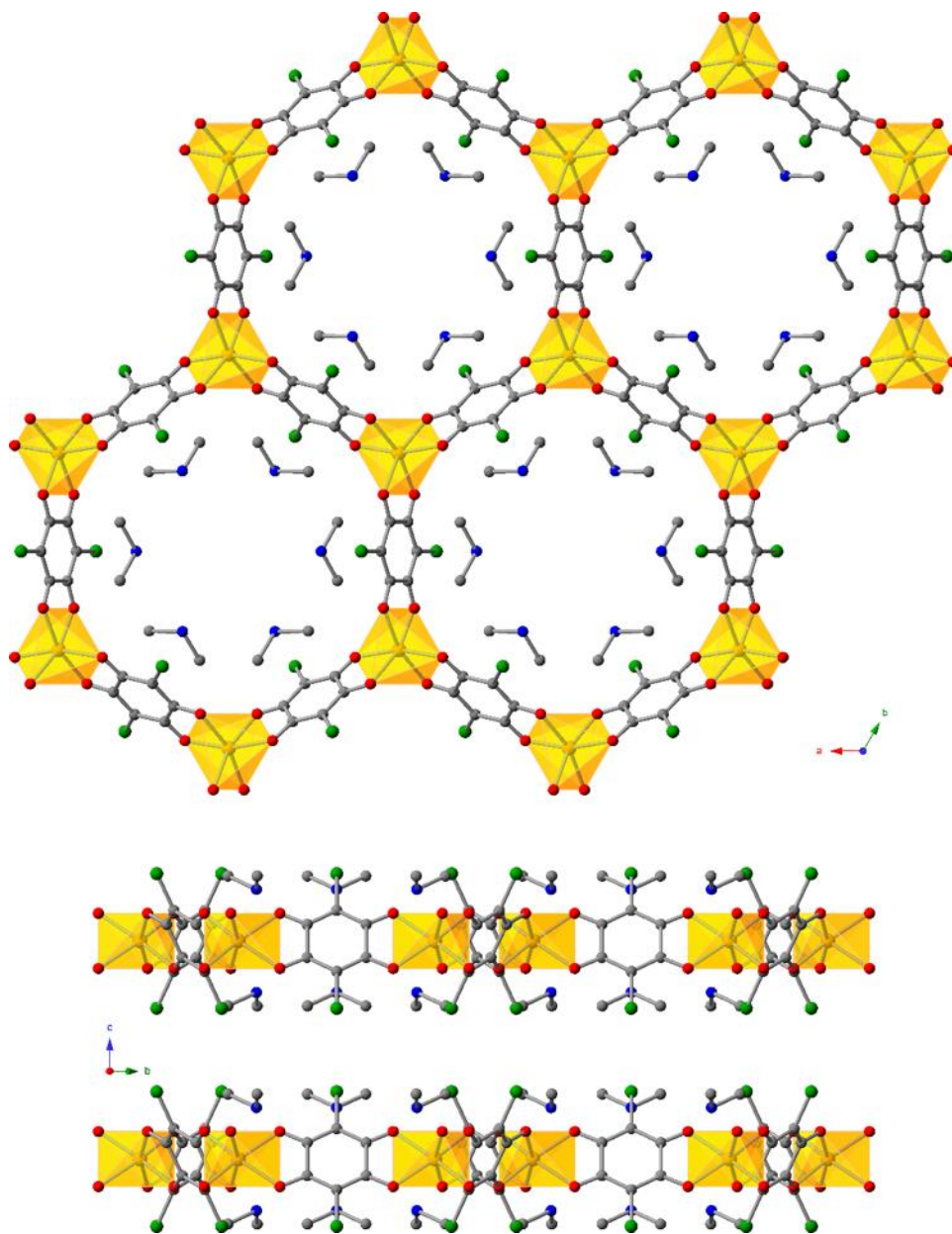
Figure S1. Single-crystal structure of $(Me_2NH_2)_2[Mn_2L_3]$ (**4**) viewed along the crystallographic *c* axis (upper) and *a* axis (lower). Orange polyhedron represents Mn atom; green, red, blue and gray spheres represent Cl, O, N, and C atoms. Solvent molecules and all hydrogen atoms are omitted for clarity. Every $Me_2NH_2^+$ counterion has an occupancy of $^1/_3$.
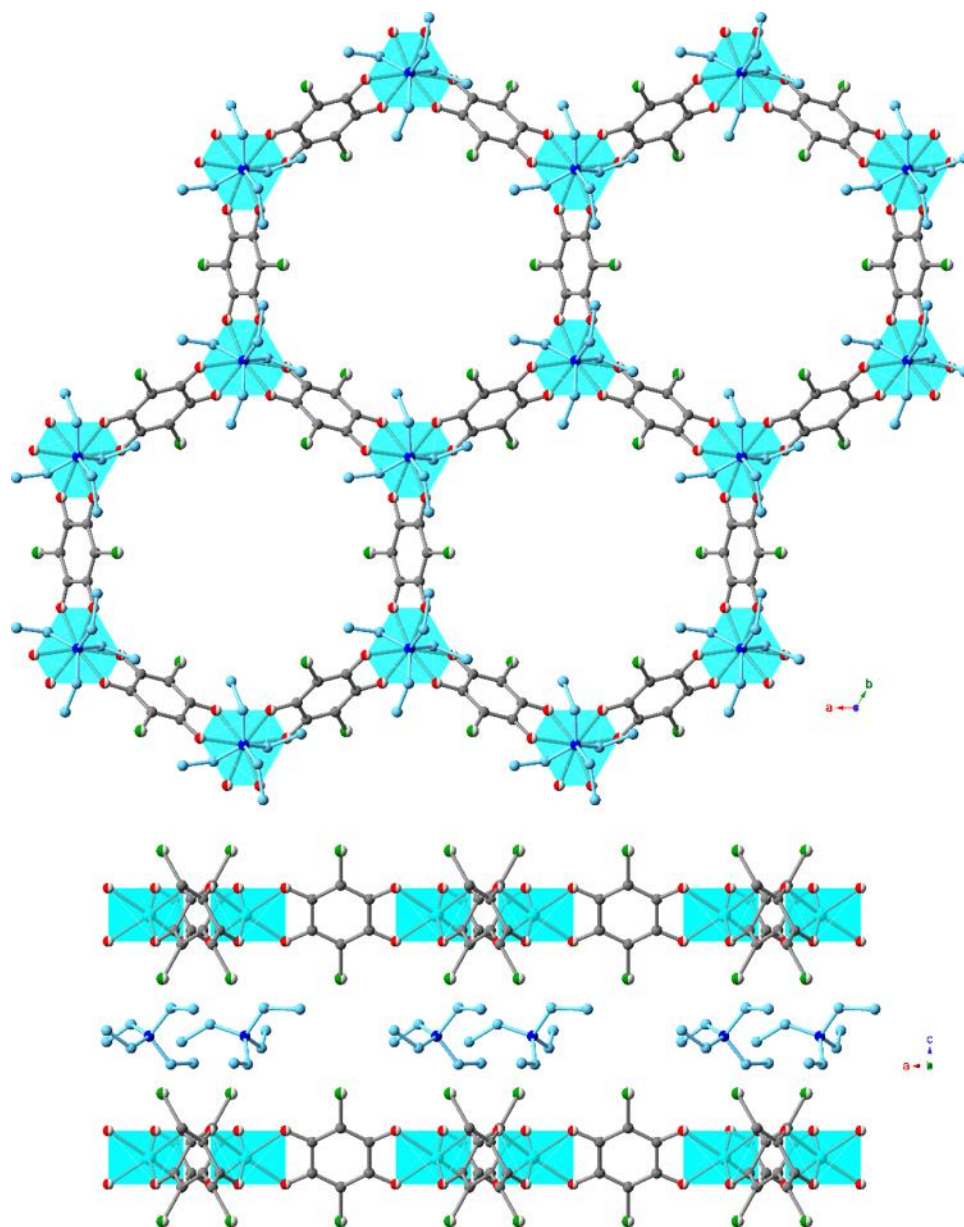
Figure S2. Single-crystal structure of $(Et_4N)_2[Zn_2L_{1.3}{}^{Br}L'_{1.7}]$ (**2**) viewed along the crystallographic *c* axis (upper) and *a* axis (lower). Cyan polyhedra represent Zn atoms; blue spheres represent N atoms; light blue and gray spheres both represent C atoms; green-white and red-white dual colored spheres represent disordered Cl/Br and O/N atoms, respectively; H atoms are omitted for clarity. The Et_4N^+ counterion is disordered and only one orientation is shown.
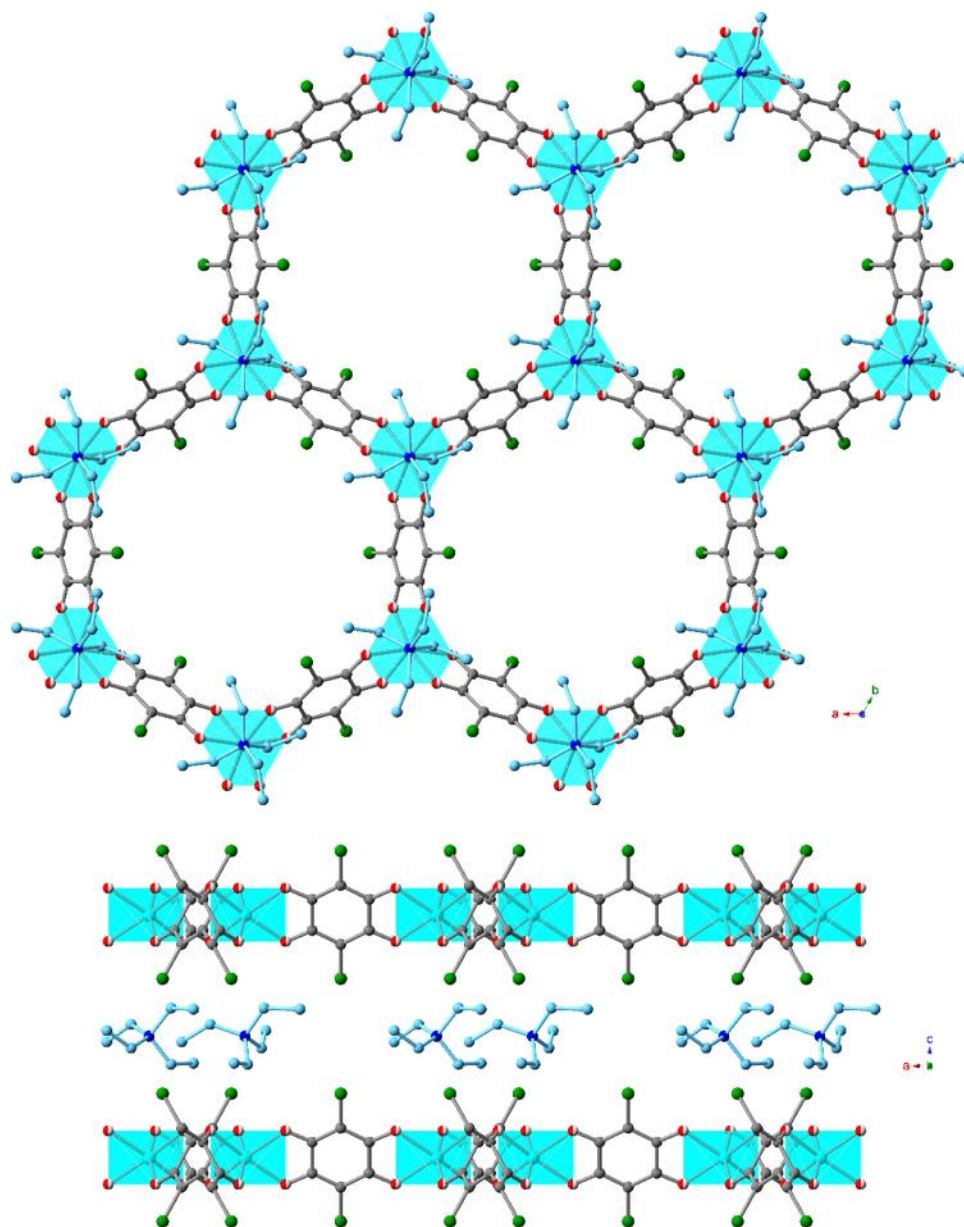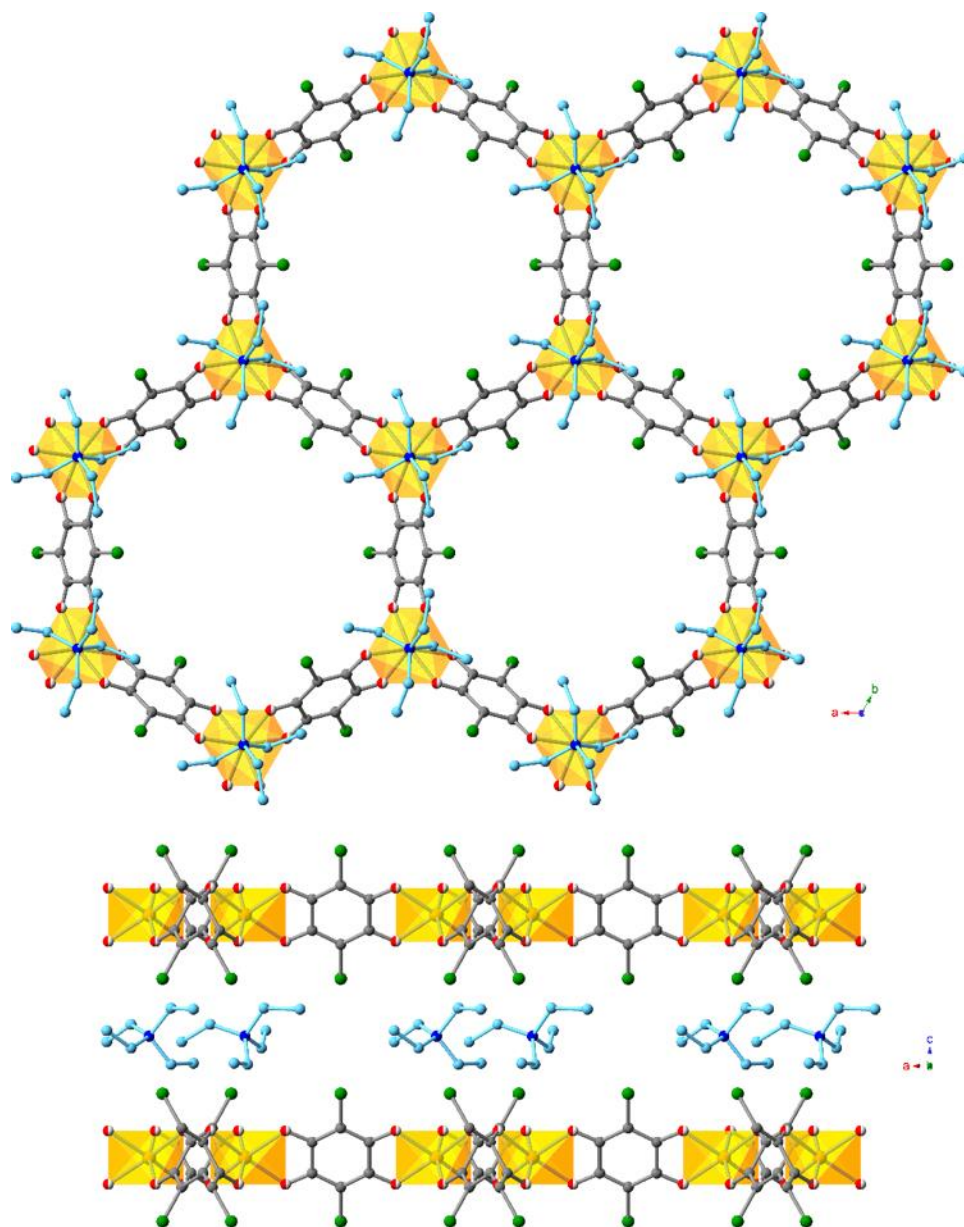
Figure S3. Single-crystal structure of $(Et_4N)_2[Zn_2L_{1.1}{}^{Cl}L'_{1.9}]$ (**3**) viewed along the crystallographic *c* axis (upper) and *a* axis (lower). Cyan polyhedra represent Zn atom; blue and green spheres represent N and Cl atoms, respectively; light blue and gray spheres both represent C atoms; red-white dual colored sphere represent disordered O/N atoms; H atoms are omitted for clarity. The Et_4N^+ counterion is disordered and only one orientation is shown.
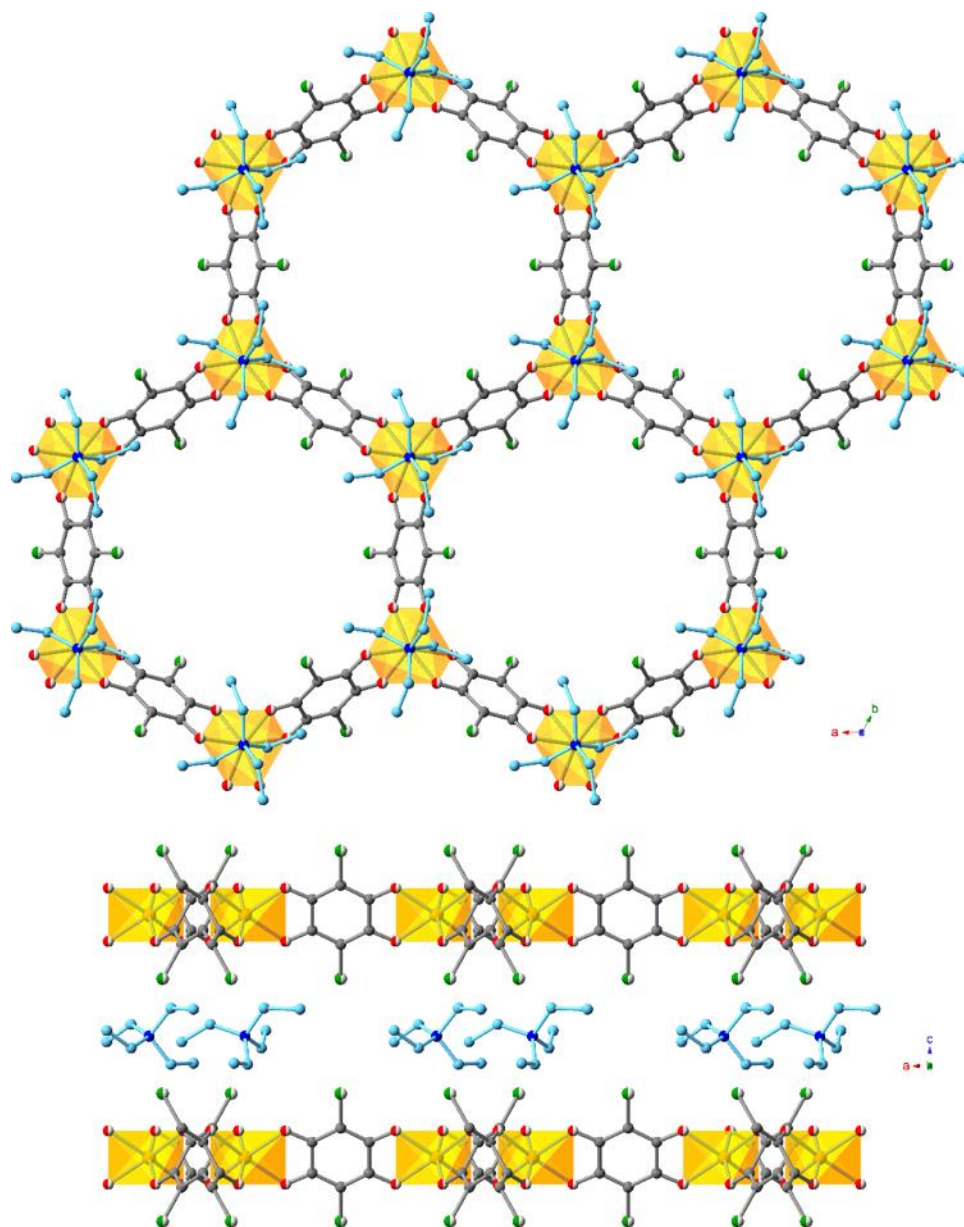
Figure S4. Single-crystal structure of $(Et_4N)_2[Mn_2L_{1.8}^{Br}L'_{1.2}]$ (**5**) viewed along the crystallographic c axis (upper) and a axis (lower). Orange polyhedra represents Mn atoms; blue spheres represents N atoms; light blue and gray spheres both represent C atoms; green-white and red-white dual colored spheres represent disordered Cl/Br and O/N atoms, respectively; H atoms are omitted for clarity. The Et_4N^+ counterion is disordered and only one orientation is shown.

Figure S5. Single-crystal structure of $(Et_4N)_2[Mn_2L_{1.5}{}^{Cl}L'_{1.5}]$ (**6**) viewed along the crystallographic *c* axis (upper) and *a* axis (lower). Orange polyhedra represent Mn atoms; blue and green spheres represent N and Cl atoms, respectively; light blue and gray spheres both represent C atoms; red-white dual colored sphere represent disordered O/N atoms; H atoms are omitted for clarity. The Et_4N^+ counterion is disordered and only one orientation is shown.
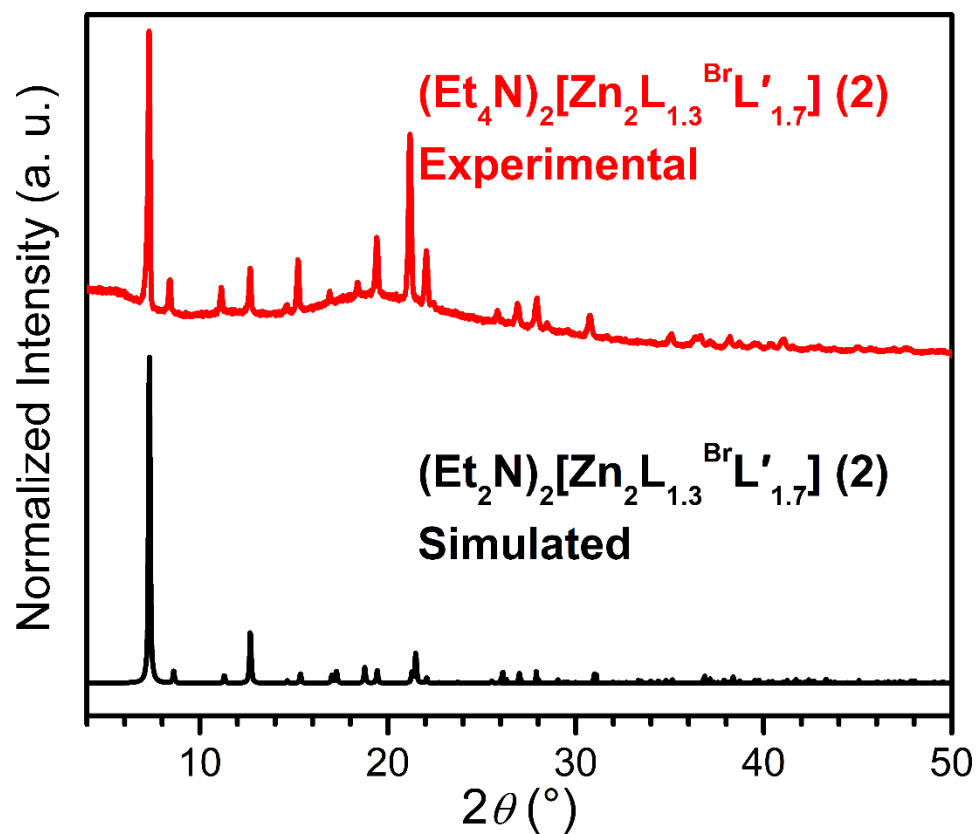
Figure S6. Experimental and simulated PXRD patterns for **2**.
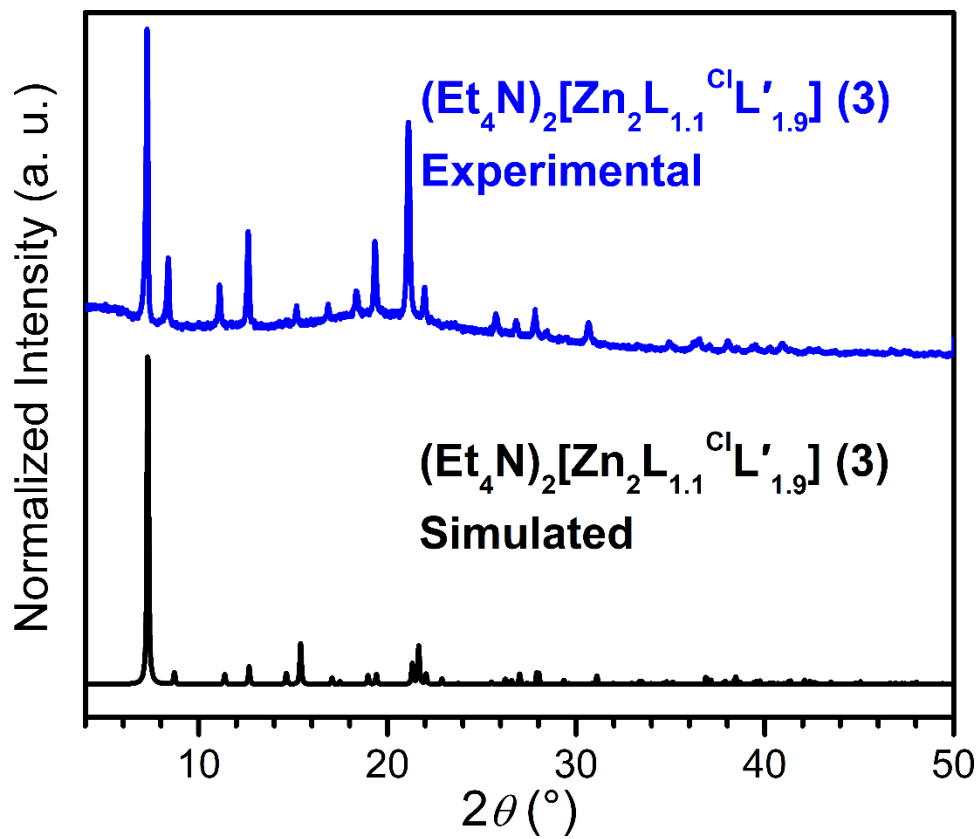
Figure S7. Experimental and simulated PXRD patterns for **3**.
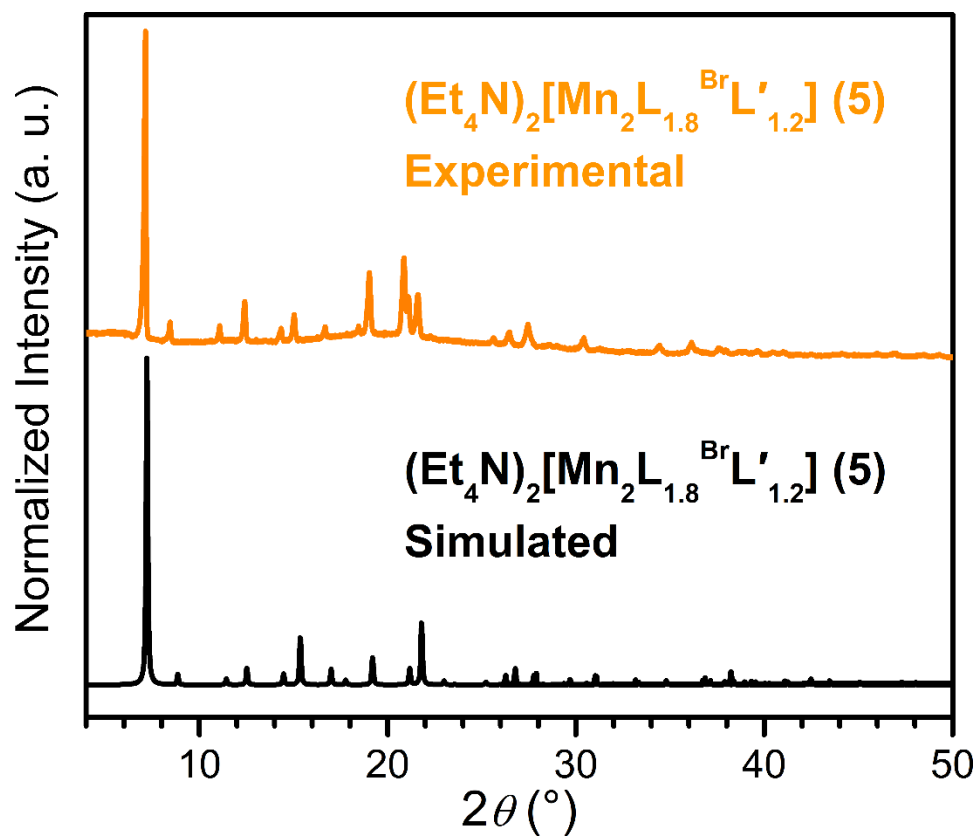
Figure S8. Experimental and simulated PXRD patterns for **5**.
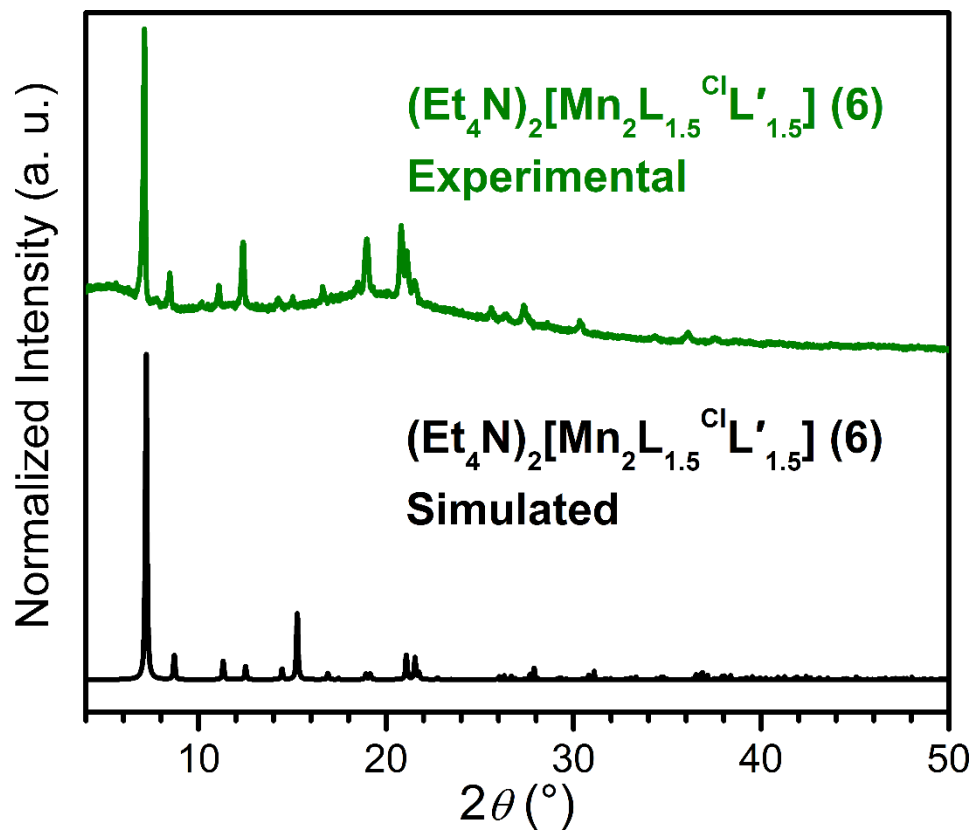
Figure S9. Experimental and simulated PXRD patterns for **6**.

LL5-017-d05.21.fid
NU_C13_1mg DMSO /home/walkon/data/Harris llz7348 51

170.12 H2BrL' (C=O)
165.78 H2L (C=O)
162.46 DMF
150.55 H2BrL' (C-N)
109.09 H2L (C-Cl)
90.17 H2BrL' (C-Br)
65.01 Et2O
51.52 Et4N+
51.49 Et4N+
51.47 Et4N+
35.91 DMF
30.89 DMF
15.25 Et2O
7.17 Et4N+

100.00
171.28
131.91
49.46
111.02

Chemical Shift (ppm)
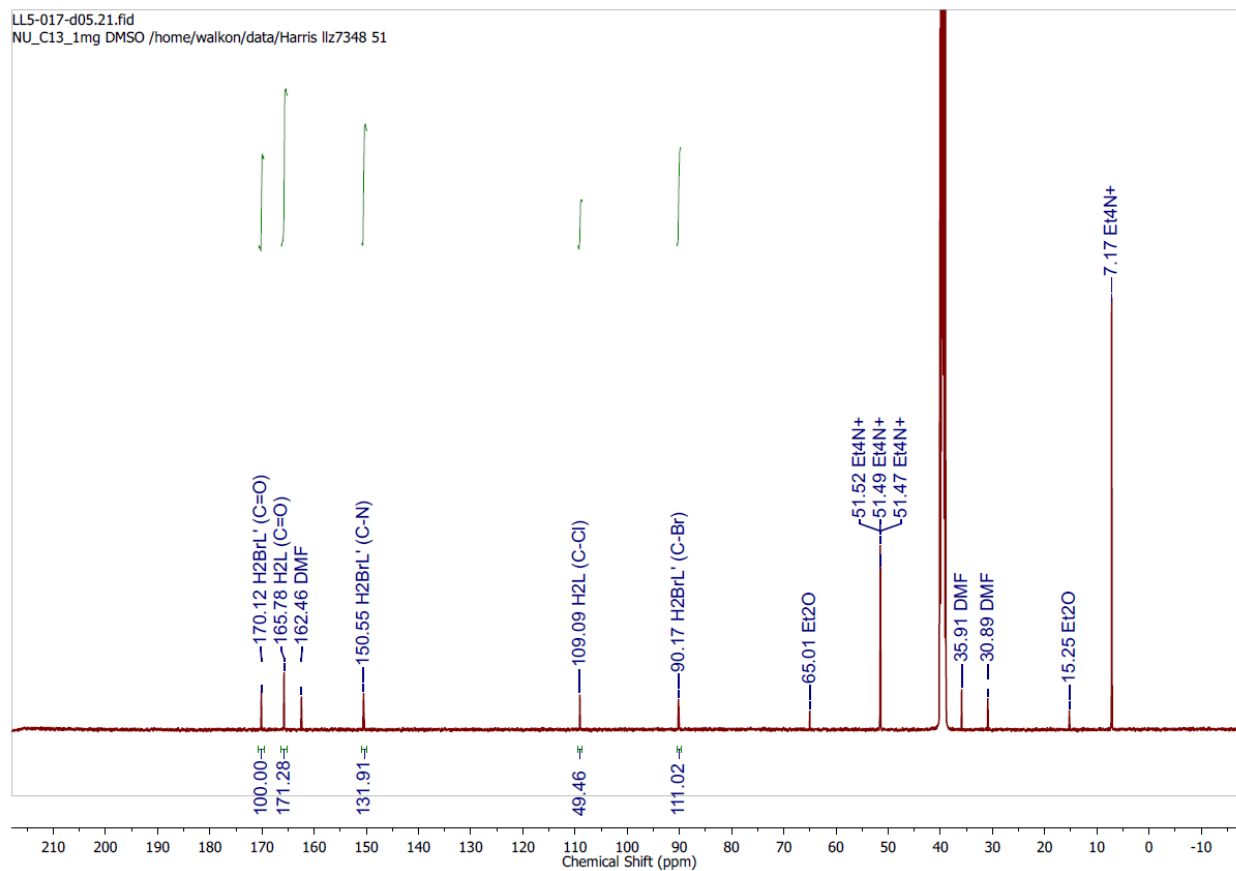
Figure S10. ^{13}C NMR spectrum for **2**.

S26

LL5-037-ACT2h.21.fid
NU_C13_1mg DMSO /home/walkon/data/Harris llz7348 50

170.13 H2ClL' (C=O)
165.69 H2L (C=O)
148.67 H2ClL' (C-N)
108.68 H2L (C-Cl)
99.41 H2ClL' (C-Cl)
54.93 DCM
51.43 Et4N+
51.41 Et4N+
51.38 Et4N+
7.11 Et4N+

100.00
98.10
113.39
41.39
65.36

Chemical Shift (ppm)
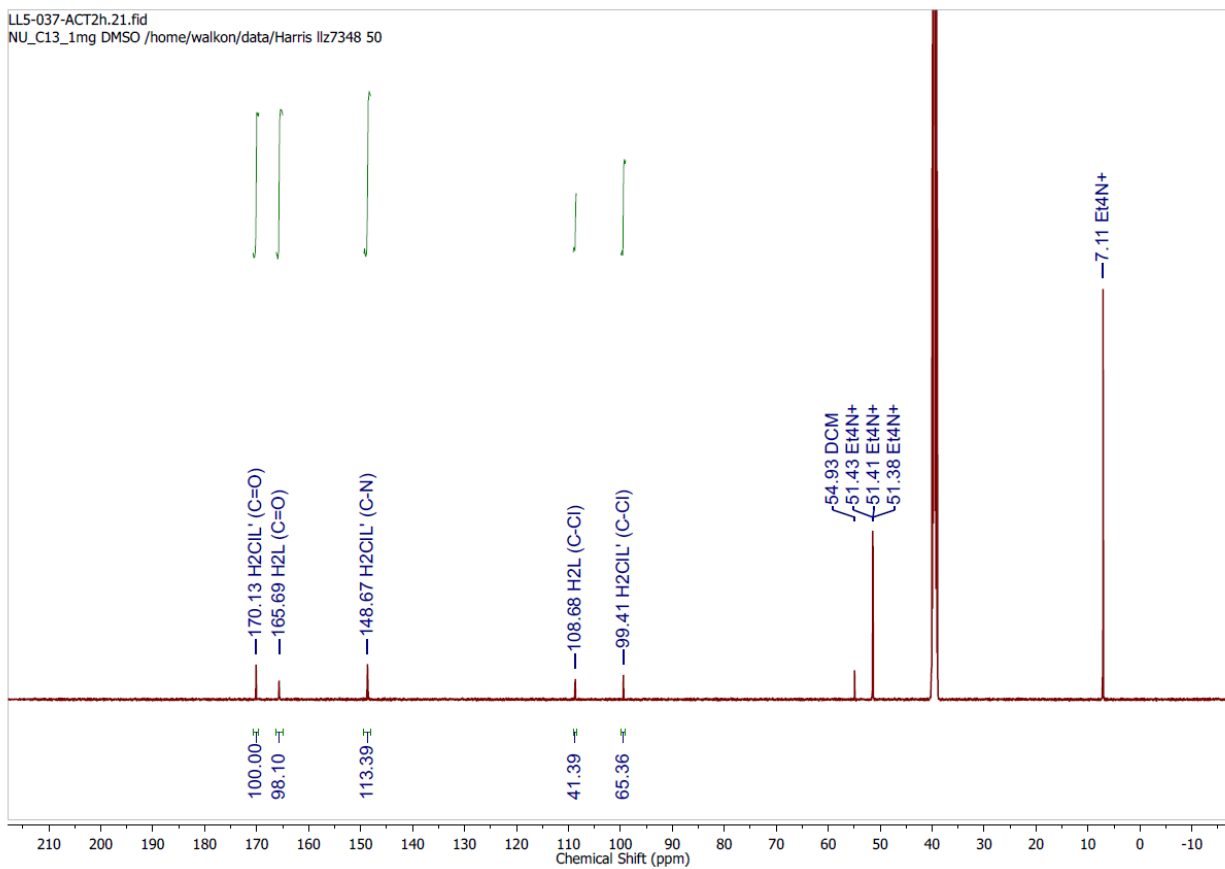
Figure S11. ^{13}C NMR spectrum for **3**.
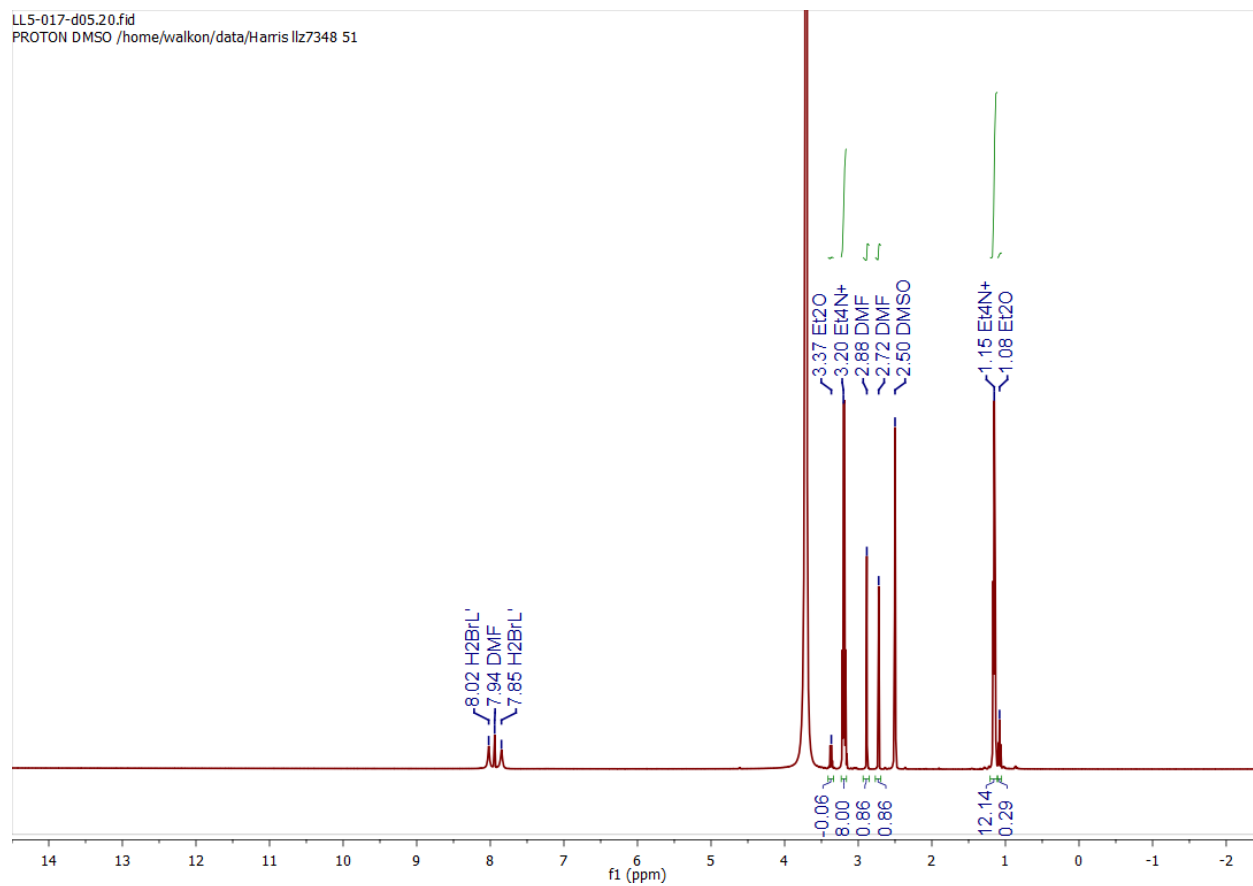
Figure S12. ^{1}H NMR spectrum for **2**.
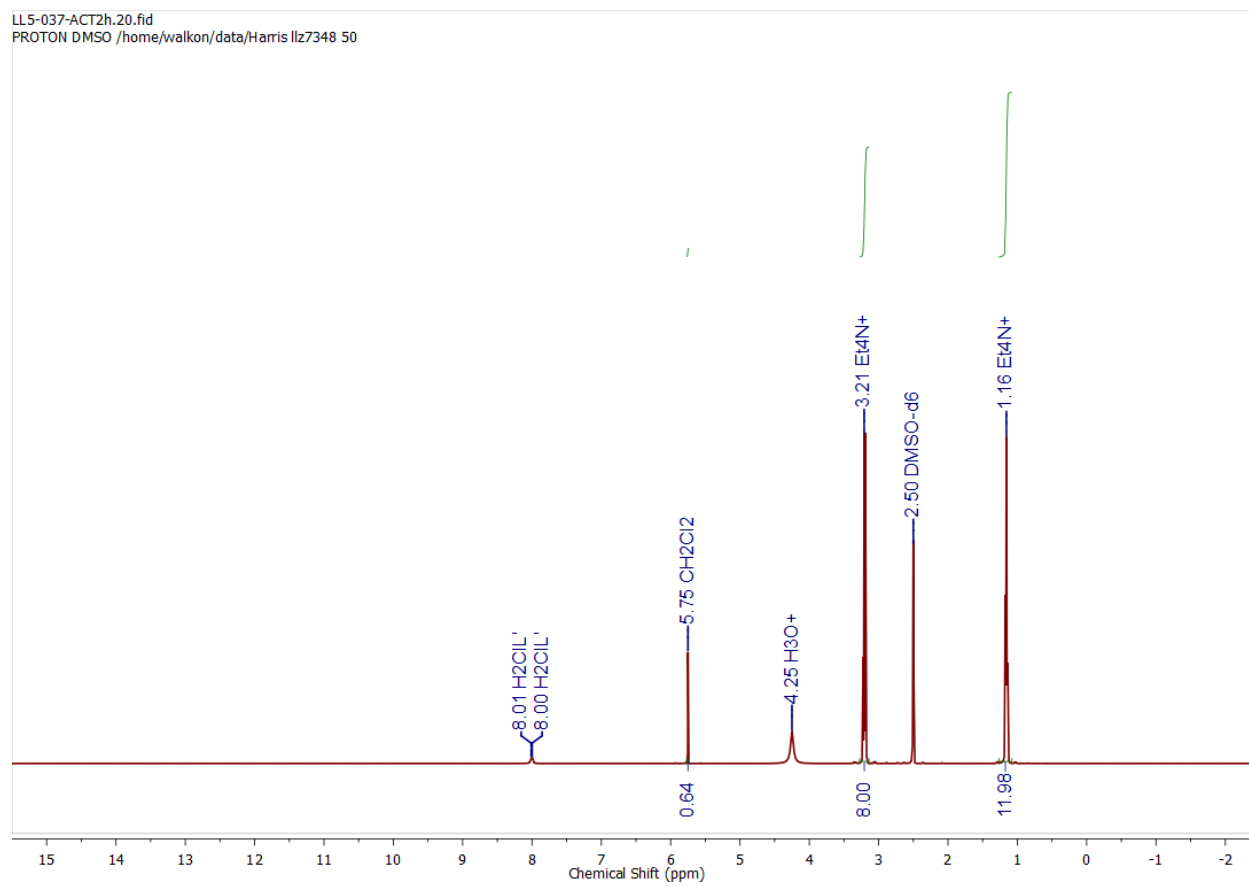
Figure S13. ^{1}H NMR spectrum for **3**.
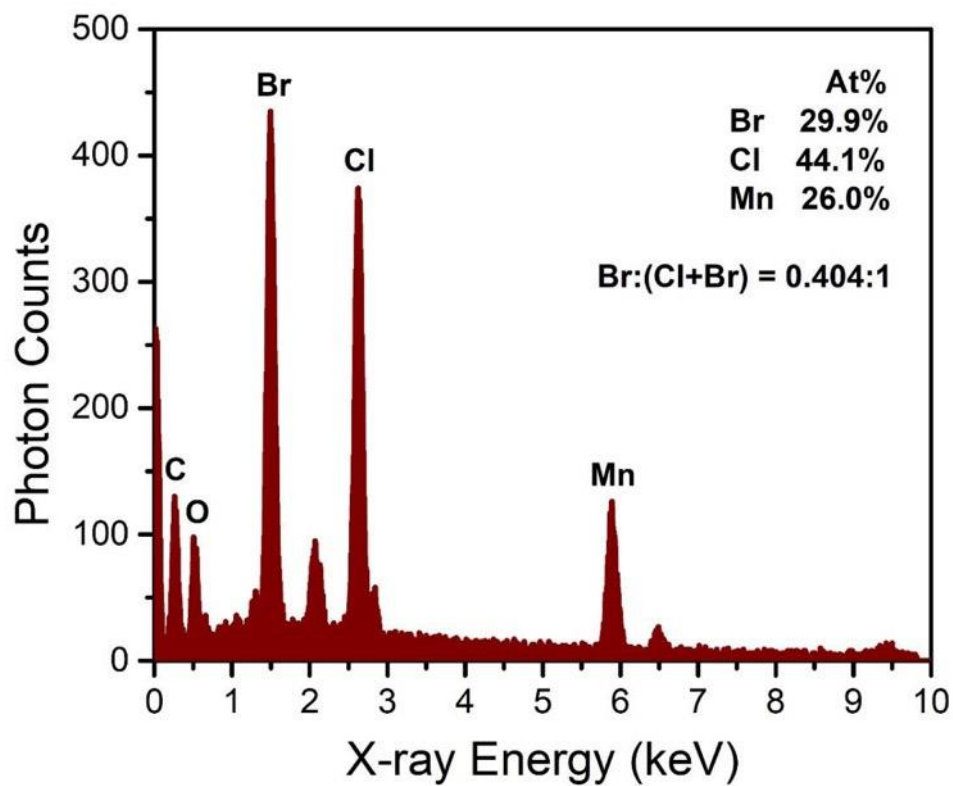
Figure S14. A representative EDX spectrum for **5**, showing a 40% linker exchange.
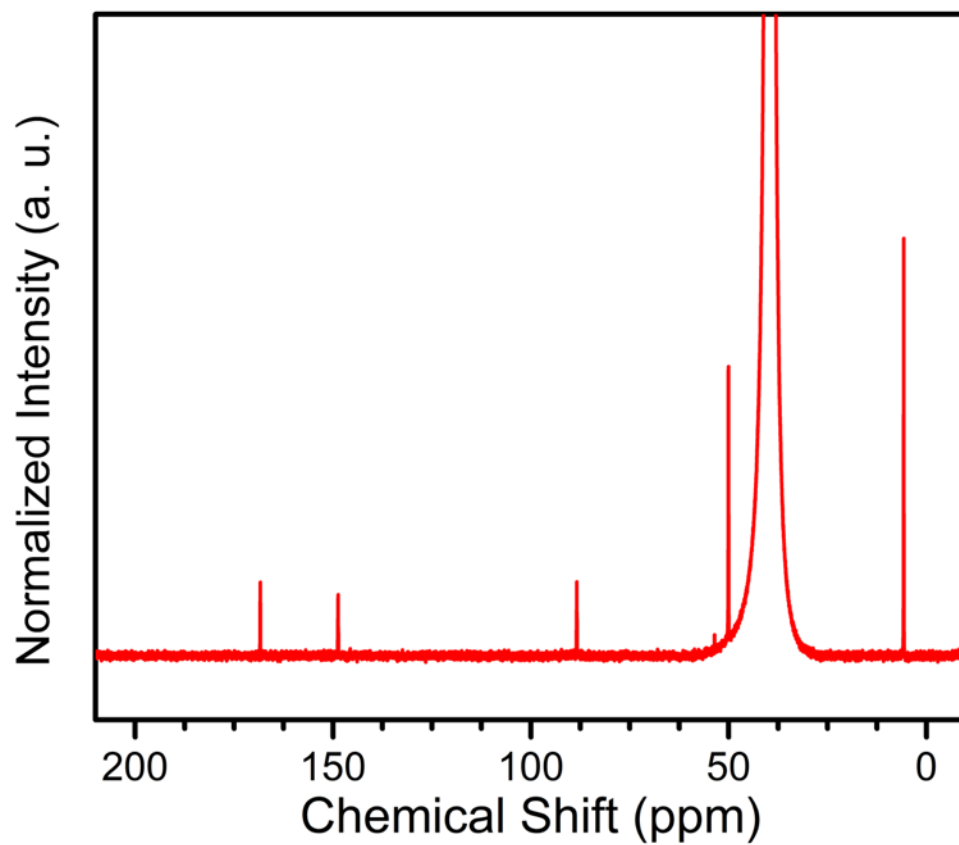
Figure S15. ^{13}C NMR spectrum for further activated sample of **5**, showing the absence of DMF. This sample was used for combustion elemental analysis.
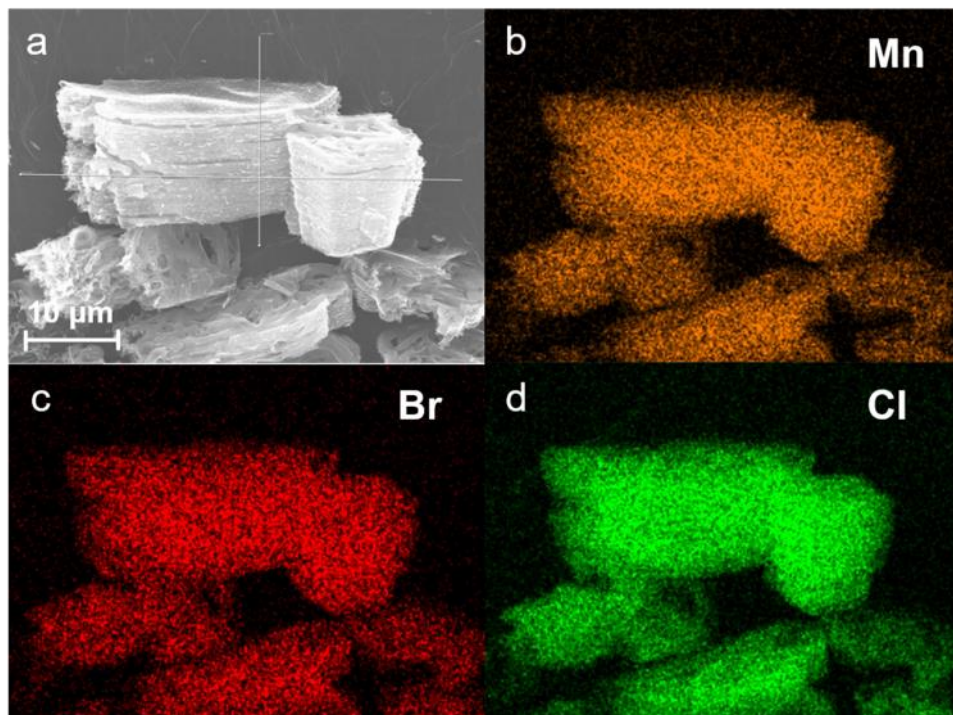
Figure S16. (a) SEM image of **5** (batch 1). (b)(c)(d) EDX mapping images with Mn, Br and Cl elements.
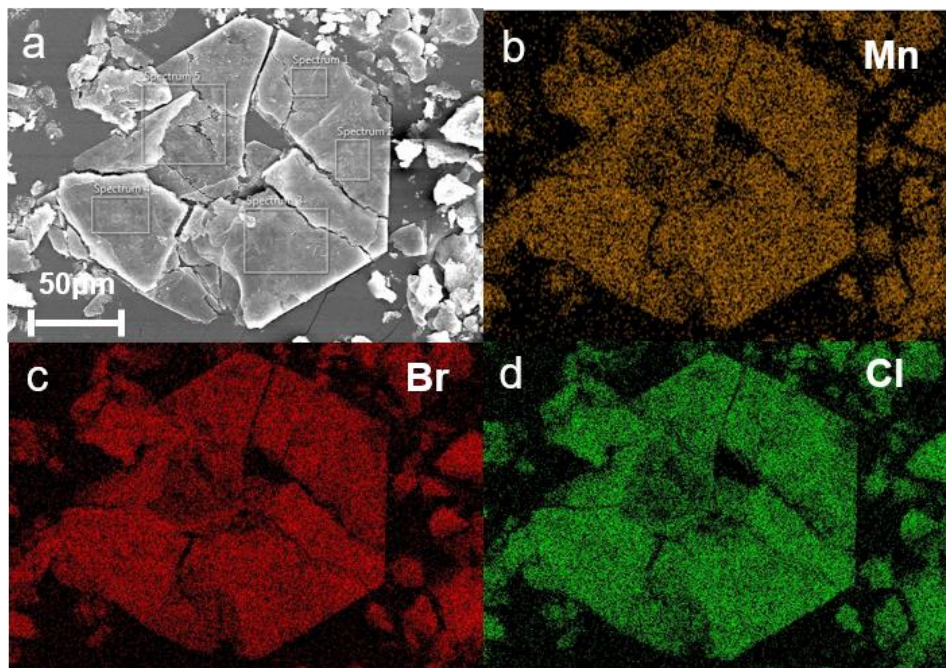
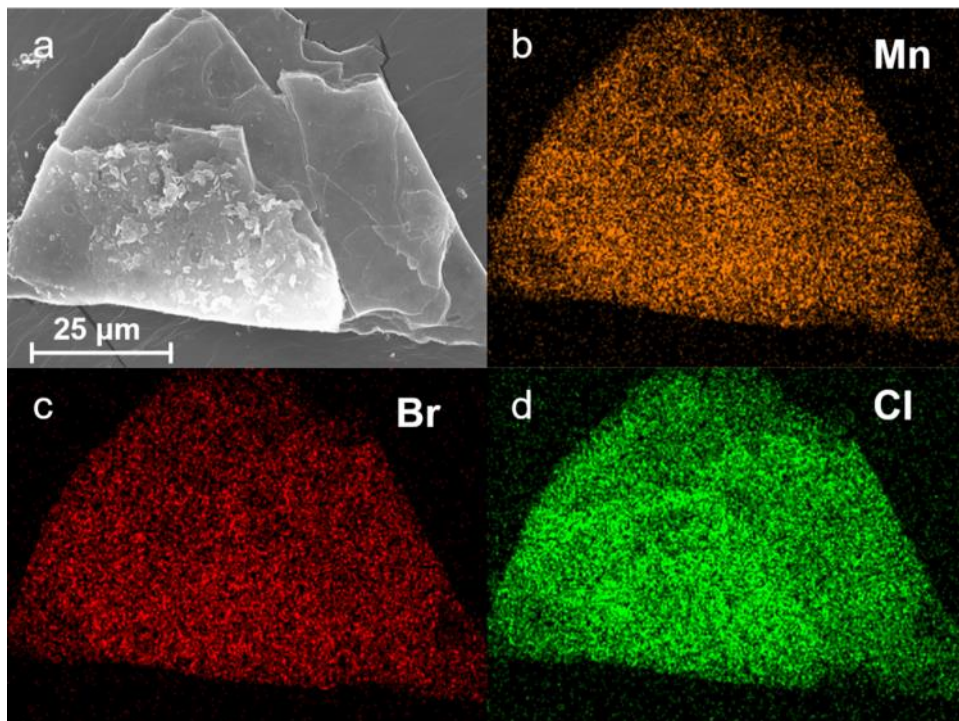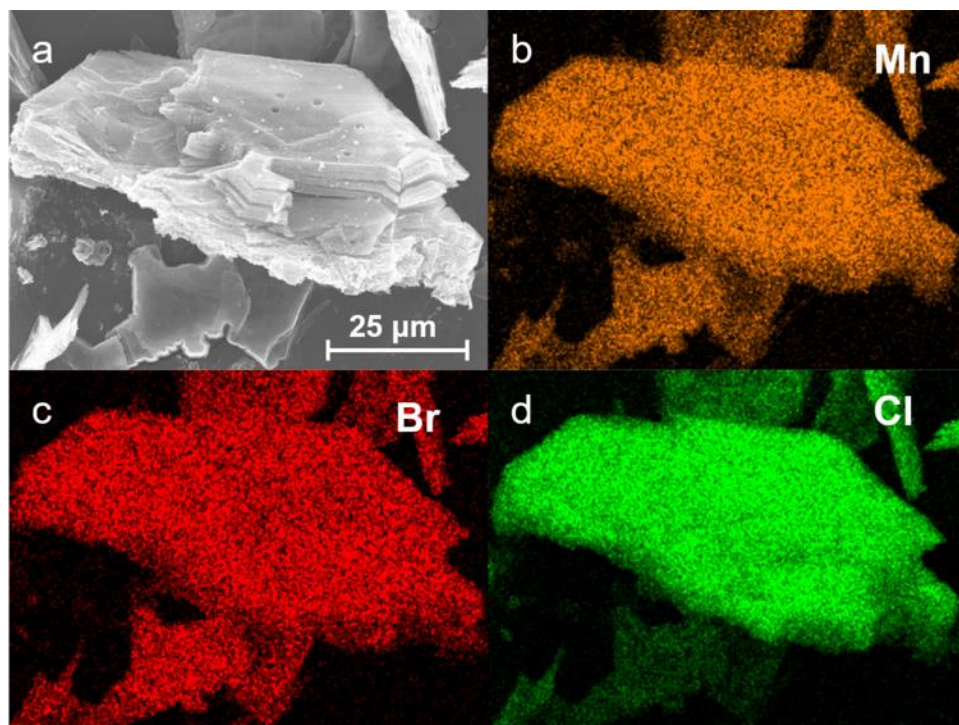**Figure S17.** (a) SEM image of **5** (batch 2). (b)(c)(d) EDX mapping images with Mn, Br and Cl elements.
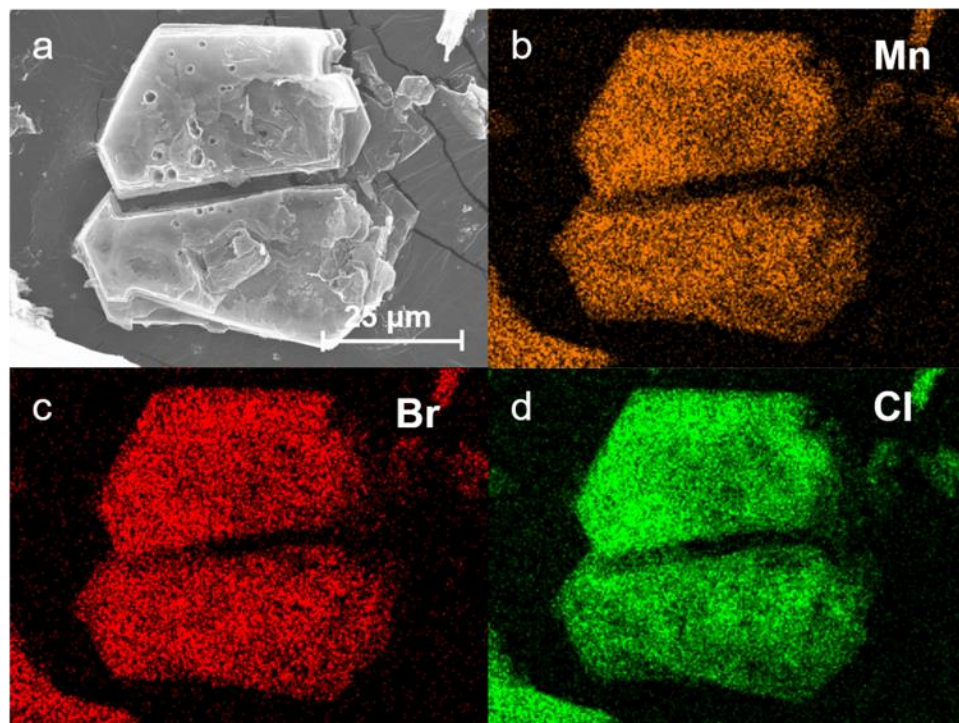
Figure S18. (a) SEM image of **5** (batch 3). (b)(c)(d) EDX mapping images with Mn, Br and Cl elements.

Figure S19. (a) SEM image of **5** (batch 4). (b)(c)(d) EDX mapping images with Mn, Br and Cl elements.

Figure S20. (a) SEM image of **5** (batch 5). (b)(c)(d) EDX mapping images with Mn, Br and Cl elements.
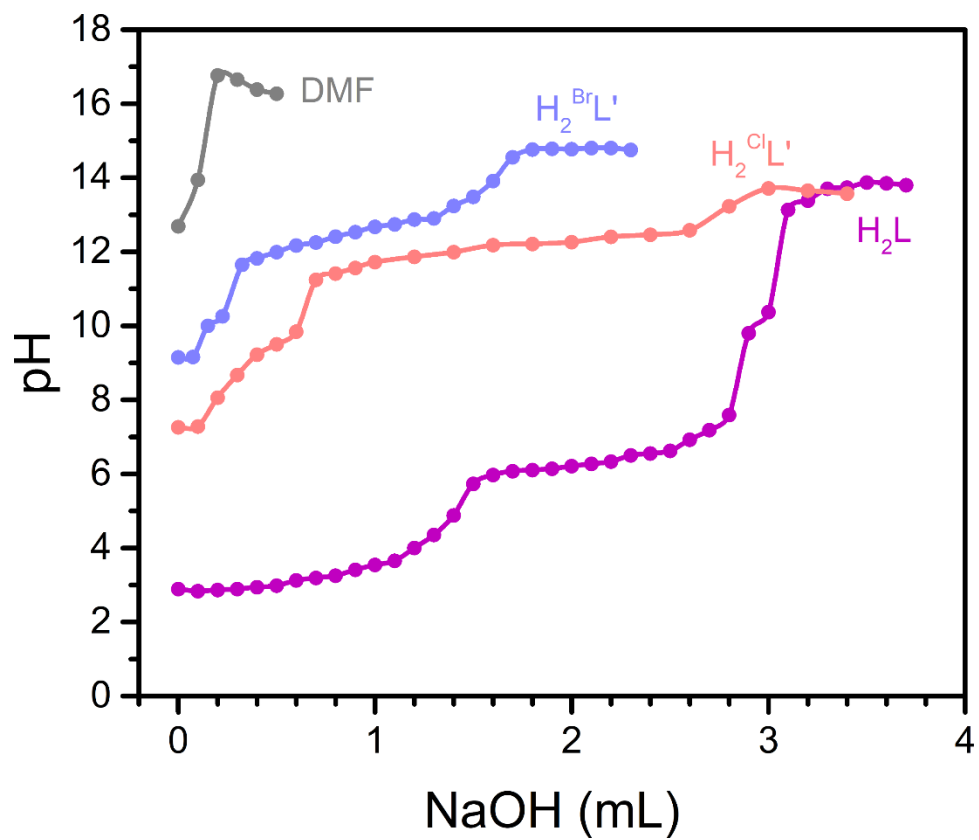
Figure S21. Acid-base titration curves for H_2L (purple), $H_2^{Br}L'$ (blue), and $H_2^{Cl}L'$ (pink). Blank curves are shown in gray.
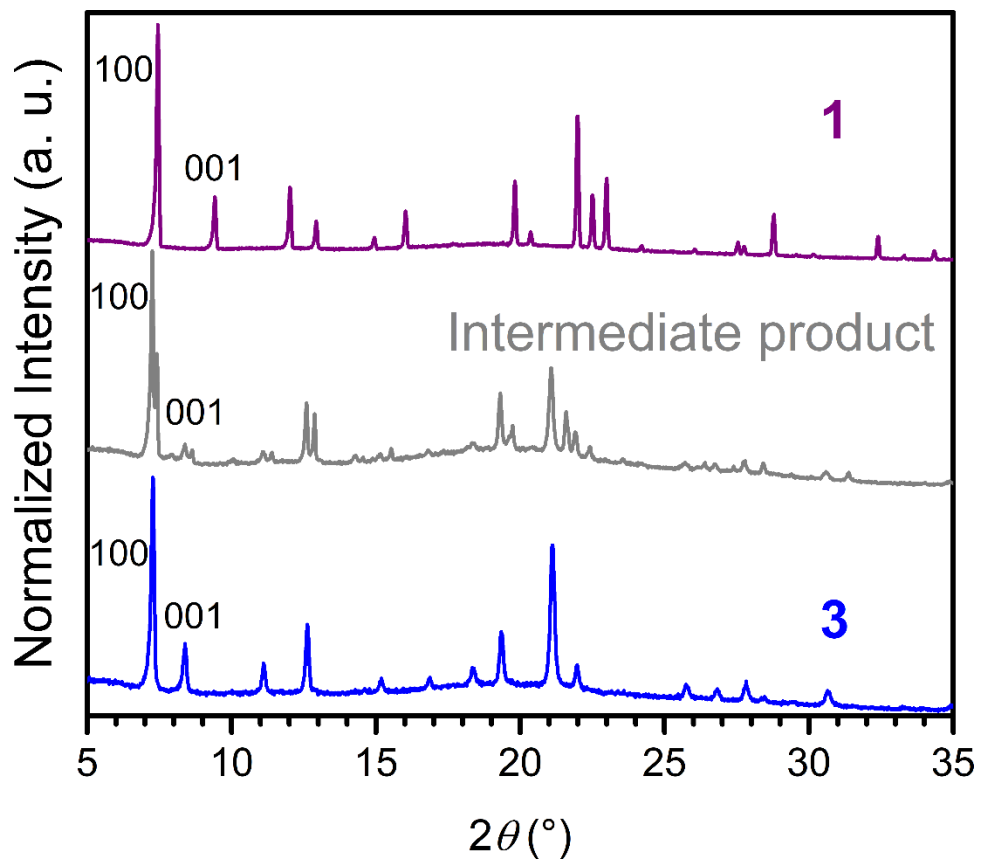
Figure S22. PXRD snapshot of an intermediate product (grey pattern) for the conversion from **1** (purple) to **3** (blue).
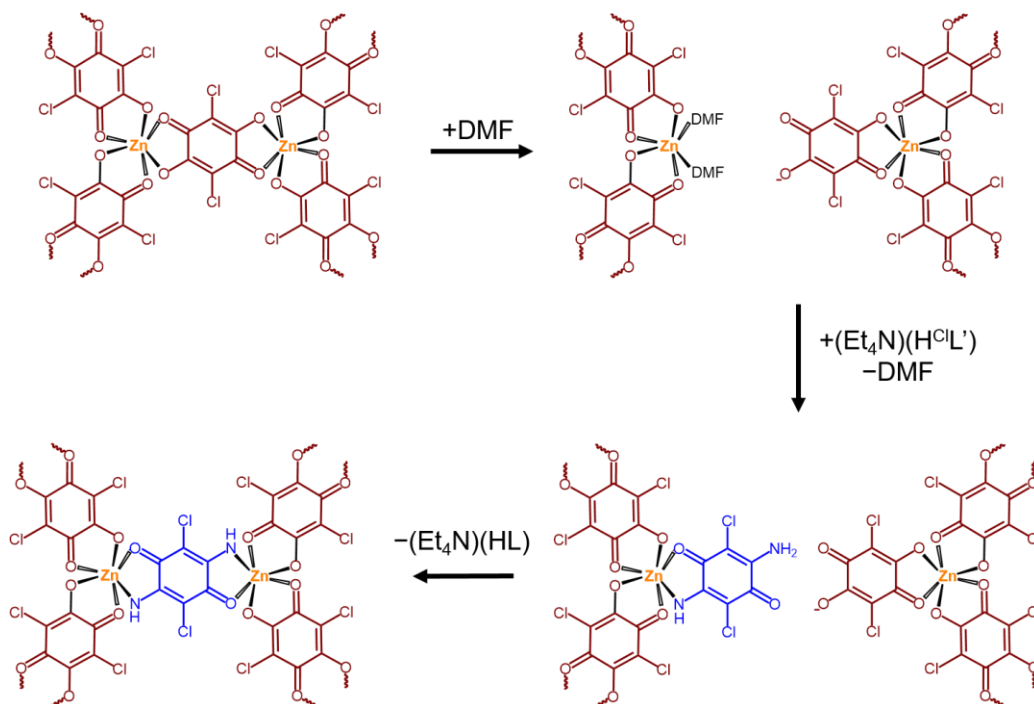
Figure S23. A proposed dissociative mechanism for linker exchange in **1**. Following dissociation of L^{2-} from one Zn ion, singly deprotonated $(H^{Cl}L')^-$ coordinates to the solvated Zn ion. Subsequent dissociation and protonolysis of L^{2-} results in formation of a bridging Zn–$(^{Cl}L')^{2-}$–Zn moiety. Note that the increases in Zn–Zn separations during the exchange are exaggerated for clarity.
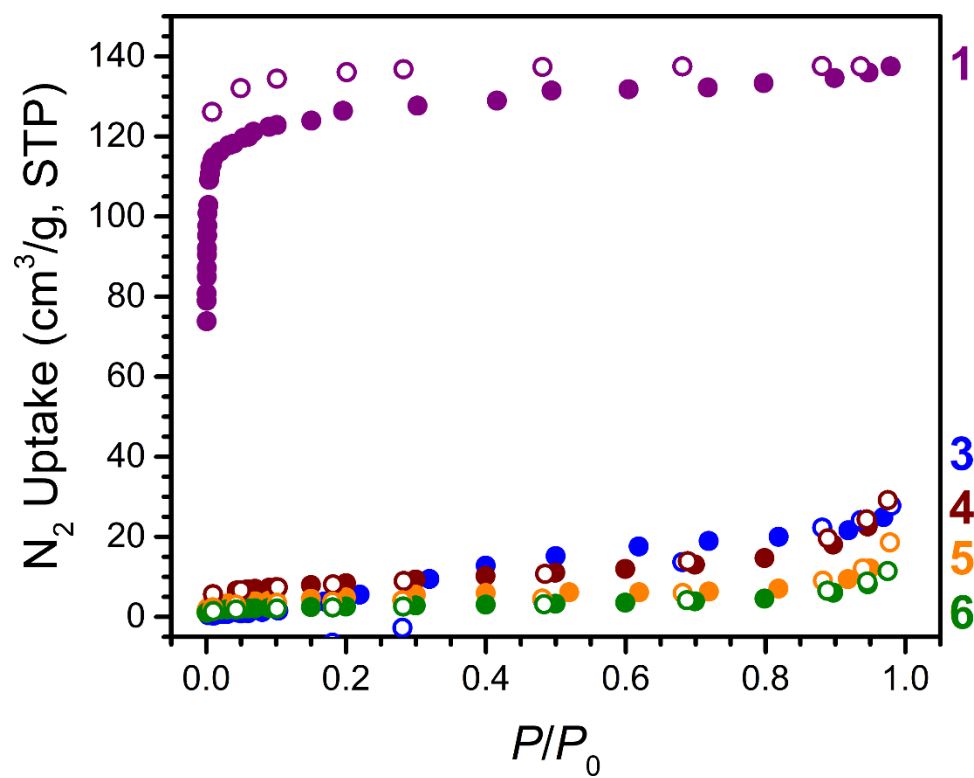
Figure S24. N_2 adsorption (filled circles) and desorption (open circles) isotherms at 77 K for **1** (purple), **3** (blue), **4** (brown), **5** (orange), and **6** (green).
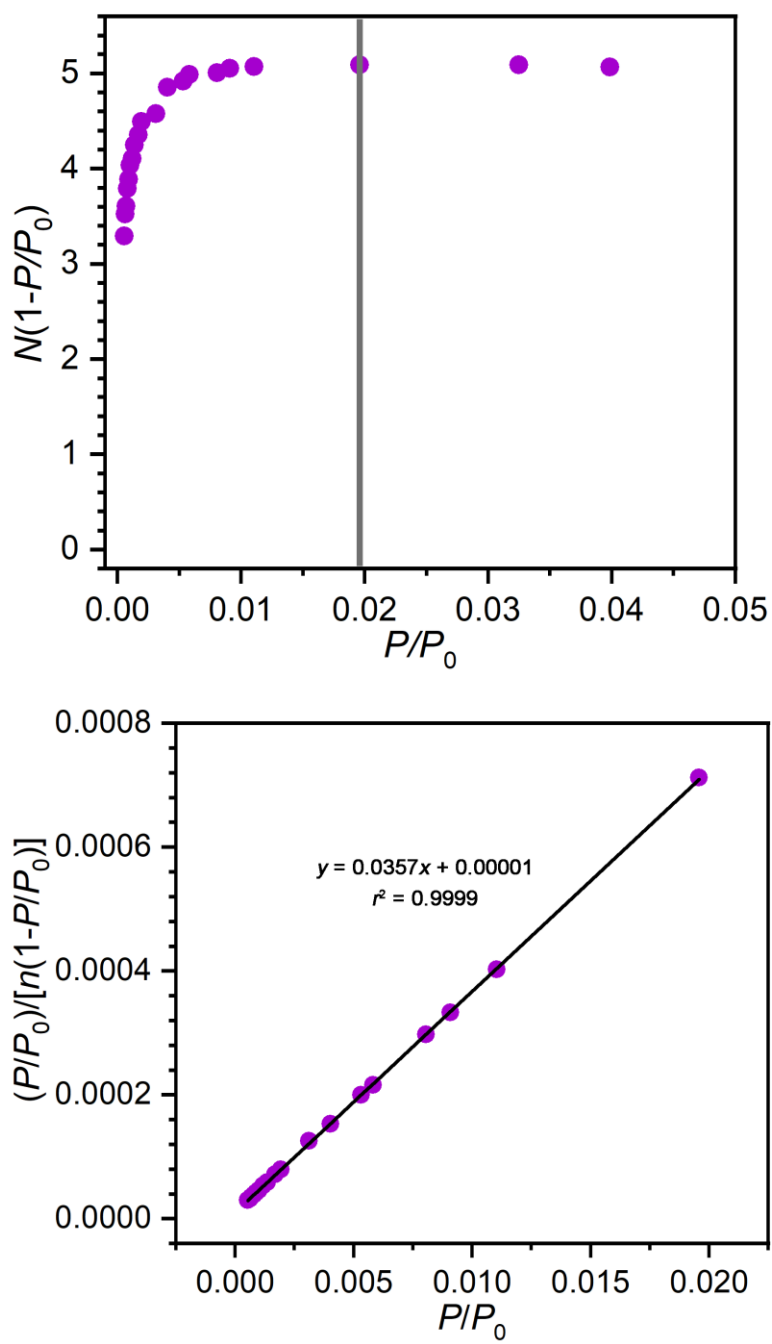
Figure S25. Consistency plots for calculating BET surface area of **1**. This yields a surface area of 610 m^2/g.[9]

References

(1)   Jeon, I.-R.; Negru, B.; Van Duyne, R. P.; Harris, T. D. *J. Am. Chem. Soc.* **2015**, *137*, 15699.

(2)   Heqedus, L. S.; Odle, R. R.; Winton, P. M.; Weider, P. R. *J. Org. Chem.* **1982**, *47*, 2607.

(3)   Inbasekaran, M.; Strom, R. *Org. Prep. Proced. Int.* **1991**, *23*, 447.

(4)   APEX 3, v. 2016.1-0; Bruker Analytical X-Ray Systems, Inc: Madison, WI, 2016.

(5)   Sheldrick, G. M. SADABS, version 2.03, Bruker Analytical X-Ray Systems, Madison, WI, 2000

(6)   Sheldrick, G.M. XPREP, version 2008/2, Bruker Analytical X-Ray Systems, Inc., Madison, WI, 2008.

(7)   Sheldrick, G. *Acta Crystallogr. A* **2008**, *64*, 112.

(8)   Dolomanov, O. V.; Bourhis, L. J.; Gildea, R. J.; Howard, J. A. K.; Puschmann, H. *J. Appl. Crystallogr.* **2009**, *42*, 339.

(9)   Walton, K. S.; Snurr, R. Q. *J. Am. Chem. Soc.* **2007**, *129*, 8552-8556.